

First Evidence for Mixing-Induced CP Violation in $B_s^0 \rightarrow J/\psi\phi(1020)$ Decays in pp Collisions at $\sqrt{s} = 13$ TeV

A. Hayrapetyan *et al.**
(CMS Collaboration)

 (Received 26 December 2024; revised 14 November 2025; accepted 30 January 2026; published 5 May 2026)

A novel machine-learning-based flavor-tagging algorithm combining same-side and opposite-side tagging is used to obtain the equivalent of 27 500 tagged $B_s^0 \rightarrow J/\psi\phi(1020)$ decays from pp collisions at $\sqrt{s} = 13$ TeV, collected by the CMS experiment and corresponding to an integrated luminosity of 96.5 fb⁻¹. A time- and flavor-dependent angular analysis of the $\mu^+\mu^-K^+K^-$ final state, consistent with a $\phi(1020) \rightarrow K^+K^-$ decay, is used to measure parameters of the $B_s^0 - \bar{B}_s^0$ system. The weak phase is measured to be $\phi_s = -73 \pm 22(\text{stat}) \pm 10(\text{syst})$ mrad, which, combined with the $\sqrt{s} = 8$ TeV CMS result, gives $\phi_s = -75 \pm 23$ mrad. This value differs from zero by 3.2 standard deviations, providing the first evidence for mixing-induced CP violation in $B_s^0 \rightarrow J/\psi\phi(1020)$ decays. All measured physics parameters are found to agree with standard model predictions where available.

DOI: 10.1103/ctqx-vxrj

The decays of B_s^0 mesons provide powerful ways to test the standard model (SM) predictions for CP violation (CPV) in the quark sector and search for new physics effects. In the SM, the weak phase ϕ_s , which arises from CPV in the interference between decays with and without mixing of B_s^0 mesons to a CP eigenstate, is related to the elements of the Cabibbo-Kobayashi-Maskawa quark mixing matrix [1,2] by $\phi_s \approx -2\beta_s = -2 \arg(-V_{ts}V_{tb}^*/V_{cs}V_{cb}^*)$, ignoring small contributions from penguin diagrams [3]. Global fits to measurements of b -hadron and kaon decays in the context of the SM predict $-2\beta_s \approx -37 \pm 1$ mrad [4,5]. This precise determination makes ϕ_s an excellent probe for beyond-the-SM physics, as its value can be modified by the contribution of new particles to B_s^0 mixing [6–8]. Several experiments have measured ϕ_s via $b \rightarrow c\bar{c}s$ transitions in B_s^0 decays [9–26], with no evident deviation from SM-based predictions. This Letter presents a study of the $B_s^0 \rightarrow J/\psi\phi(1020)$ decay to the $\mu^+\mu^-K^+K^-$ final state using proton-proton collisions collected by the CMS experiment [27,28] at $\sqrt{s} = 13$ TeV during 2017–2018, corresponding to an integrated luminosity of 96.5 fb⁻¹ [29–31]. Data collected in 2016 are not used as they were collected with a different inner tracker detector and trigger strategies. This analysis not only introduces a pioneering flavor-tagging

algorithm and incorporates additional trigger paths compared to Ref. [15], but also features a comprehensively reworked and improved analysis procedure, ultimately yielding the largest effective number of tagged signal candidates ever used for a single measurement of ϕ_s . A combination of this result with the one obtained by CMS at $\sqrt{s} = 8$ TeV [14] is also presented. In this Letter, wherever a particle or its decay mode is specified, the charge conjugate is also implied unless otherwise indicated.

The $B_s^0 \rightarrow J/\psi\phi(1020)$ decay proceeds through a mixture of CP eigenstates, which requires an amplitude analysis to separate the CP -odd and CP -even components. A time-dependent angular analysis is performed in the transversity basis [32] by measuring the decay angles of the final-state particles $\Theta = (\theta_T, \psi_T, \varphi_T)$ and ct , which is the proper decay time of the reconstructed B_s^0 meson candidate, as described in Refs. [15,33]. In the transversity basis, a reference frame is chosen such that the x axis aligns with the $\phi(1020)$ momentum, and the x - y plane is the $\phi(1020) \rightarrow K^+K^-$ decay plane. The polar and azimuthal angles of the μ^+ in the J/ψ rest frame are denoted θ_T and φ_T , respectively. The helicity angle ψ_T , computed in the $\phi(1020)$ rest frame, is the angle between the K^+ momentum and the direction of negative J/ψ momentum. The three decay angles are illustrated in Fig. 1 (left). The decay rate formalism used to describe the distribution of final-state particles is the same as in previous CMS results [14,15]. The CPV in the $B_s^0 - \bar{B}_s^0$ system is described by the complex parameter $\lambda = (q/p)(\bar{A}_f/A_f)$, where A_f (\bar{A}_f) is the decay amplitude of the B_s^0 (\bar{B}_s^0) meson to the final state f , and the parameters p and q relate the heavy and light mass eigenstates to the flavor eigenstates through $B_s^{L(H)} = p|B_s^0\rangle_{(-)} + q|\bar{B}_s^0\rangle$ [34]. The parameters of interest

*Full author list given at the end of the Letter.

Published by the American Physical Society under the terms of the Creative Commons Attribution 4.0 International license. Further distribution of this work must maintain attribution to the author(s) and the published article's title, journal citation, and DOI. Funded by SCOAP³.

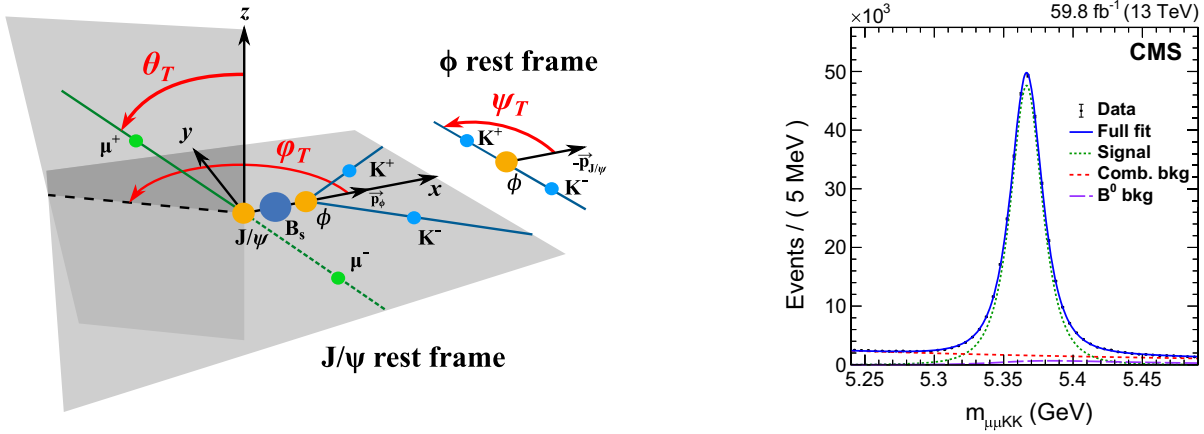


FIG. 1. Left: definition of the three decay angles θ_T , ψ_T , and ϕ_T . Right: invariant mass distribution and fit projection of the selected candidates for the ST trigger category (2018 data).

(POI) describing the decay rate are the weak phase ϕ_s ; the decay width and absolute mass differences between the B_s^0 mass eigenstates $\Delta\Gamma_s$ and Δm_s ; their average decay width Γ_s ; the direct CPV observable $|\lambda|$; the longitudinal, parallel, and perpendicular transversity amplitudes A_0 , A_{\parallel} , and A_{\perp} ; and the corresponding (CP conserving) strong phases δ_0 , δ_{\parallel} , and δ_{\perp} . Possible contributions from $B_s^0 \rightarrow J/\psi f_0(980)$ and nonresonant $B_s^0 \rightarrow J/\psi K^+K^-$ decays are taken into account by including an additional S -wave term in the decay model, parametrized with amplitude A_S and phase δ_S . An effective coupling factor is required to model the S - P -wave interference due to the lack of an $m(K^+K^-)$ parametrization in the fit model. Within the $m(K^+K^-)$ range used in this analysis (1009.5–1029.5 MeV), we calculate this correction to be $k_{\text{SP}} = 0.538 \pm 0.004$ by integrating the mass line shape interference term. A relativistic Breit-Wigner distribution and a constant distribution are assumed to describe the P and S wave, respectively, with a Flatté distribution [35] used as an alternative assumption to estimate the k_{SP} uncertainty. The strong phase δ_0 is selected as the reference phase and set to zero, following a general convention [10,12]. The value of $\Delta\Gamma_s$ is constrained to be positive, based on Ref. [36]. To reduce correlations, $\delta_{S\perp} \equiv \delta_S - \delta_{\perp}$ is used instead of δ_S . Possible $B_s^0 - \bar{B}_s^0$ production asymmetries are neglected, as the effect is expected to be small and below the sensitivity of the analysis, consistent with what is typically done in measurements of this type.

The CMS apparatus is a multipurpose, nearly hermetic detector, designed to perform a wide range of particle physics measurements. The $B_s^0 \rightarrow J/\psi\phi(1020) \rightarrow \mu^+\mu^-K^+K^-$ data sample (“ B_s^0 data sample”) is collected with two independent triggers [37]. The first trigger (“muon-tagging,” MT) requires a $J/\psi \rightarrow \mu^+\mu^-$ candidate along with an additional muon, potentially usable for flavor tagging [14]. In the second trigger (“standard,” ST), events with a displaced $J/\psi \rightarrow \mu^+\mu^-$ candidate in conjunction with a

$\phi(1020) \rightarrow K^+K^-$ vertex are demanded. To avoid double counting, events collected by the MT trigger are not considered in the ST trigger. To improve the signal purity, additional selection requirements are applied, including a requirement of $ct > 60(100) \mu\text{m}$ for the MT (ST) triggered events. A total of 67 908 and 555 213 candidates are selected from the MT and ST triggered events, respectively. The distributions for the invariant mass $m_{\mu\mu KK}$, ct , and its uncertainty σ_{ct} of the selected candidates in the ST trigger category (2018 data) are shown in Figs. 1 (right) and 2 (left and center). Appendixes A and B provide a more detailed description of the experimental setup and event reconstruction, while distributions for the other data samples can be found in Supplemental Material [38].

The flavor of the B_s^0 meson candidate, i.e., its particle or antiparticle state at production, is determined using a novel flavor-tagging framework developed for this measurement. It consists of four separate tagging algorithms (“taggers”): opposite-side (OS) muon, OS electron, OS jet, and same side (SS). The OS taggers infer the flavor of the b quark contained in the signal b meson by exploiting the decay products of the other b quark in the event, relying on the fact that b quarks are predominantly produced in $b\bar{b}$ pairs. The SS tagger takes advantage of the charge correlations between the b quark in the signal b meson and nearby particles produced in its hadronization, which reflect the underlying flavor content. Each tagging algorithm produces a tagging inference $\xi_{\text{tag}} = 0, +1, -1$, indicating whether the event is untagged, tagged as B_s^0 or \bar{B}_s^0 . For tagged events, the algorithm also estimates the mistag probability ω_{tag} . The tagging efficiency (ϵ_{tag}) represents the fraction of tagged events, while the dilution factor $\mathcal{D}_{\text{tag}} \equiv 1 - 2\omega_{\text{tag}}$ quantifies the inference purity. The tagging power $P_{\text{tag}} \equiv \epsilon_{\text{tag}}\mathcal{D}_{\text{tag}}^2$ combines these parameters and reflects the effective number of correctly tagged signal events ($N_{B_s^0}P_{\text{tag}}$), contributing to flavor-sensitive measurements.

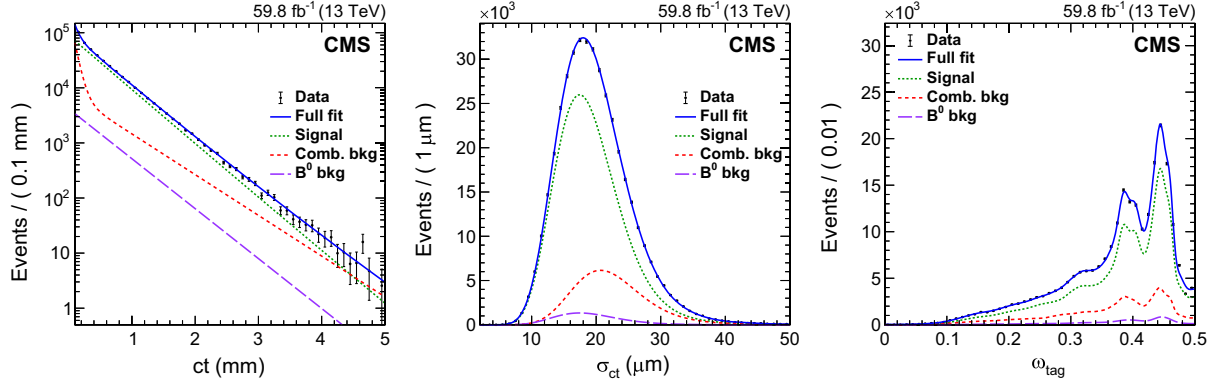


FIG. 2. Distributions of the proper decay time ct , its uncertainty σ_{ct} , and mistag probability ω_{tag} of the selected candidates for the ST trigger category (2018 data). The projections of the fitted model are also shown.

All four taggers are used for the ST datasets, while only the OS muon algorithm is used in the MT ones. The OS taggers are designed to be orthogonal to each other, meaning only one can provide an inference for each event. To improve performance, ω_{tag} is estimated on a per-event basis by dedicated deep neural networks (DNNs) developed using simulated events and calibrated in data. For the OS jet and SS taggers, the same DNNs are also used to infer ξ_{tag} . These calibrated DNNs act as probability estimators for the tagging inference. When an OS and the SS algorithm both provide tagging inferences, ξ_{tag} and ω_{tag} are recalculated by combining the available information. Appendix B provides more details about the tagging algorithms.

The combined tagging performance for the B_s^0 data sample is $\epsilon_{\text{tag}} \approx 56\%$ and $P_{\text{tag}} \approx 5.6\%$. The performance breakdown in each mutually exclusive tagging category is reported in Table III. The mistag probability distribution of the selected candidates for the ST trigger category (2018 data) is shown in Fig. 2 (right).

The flavor tagging is validated with extensive studies on simulated data and $B^0 \rightarrow J/\psi K^*(892)^0 \rightarrow \mu^+ \mu^- K^+ \pi^-$ events (“ B^0 control data sample”). Several measurements are performed on this sample to ensure that the tagging inference is reliable and free from significant bias. To test the robustness of the tagging framework in mixing scenarios, B^0 flavor oscillations are analyzed. Using the tagging framework, the fitted value of the oscillation frequency is $\Delta m_d = 0.5081 \pm 0.0046(\text{stat}) \hbar \text{ps}^{-1}$, which is in excellent agreement with the world-average value of $0.5069 \pm 0.0019 \hbar \text{ps}^{-1}$ [33]. The time-integrated mixing asymmetry in the B^0 control data sample is also examined, to investigate possible issues with the overall tagging calibration scale of the SS tagger. This is done by comparing the relationship between the measured mixing asymmetry and the estimated tagging dilution. The observed experimental dilution is found to be consistent with the estimated value. All validation studies are conducted using each

tagger independently and in each tagging category, as well as using the tagging inference from the overall framework. Moreover, the CPV measurement in the $B_s^0 \rightarrow J/\psi \phi(1020)$ channel is repeated four additional times, each using only one of the four tagging algorithms, and the obtained results are compared. No evidence of bias has been found in any of the studies.

The B_s^0 data are divided into four main datasets according to the two trigger categories and two data taking years and further divided into a total of 12 datasets based on the three possible values of ξ_{tag} . The POI ϕ_s , $\Delta\Gamma_s$, Γ_s , Δm_s , $|\lambda|$, $|A_0|^2$, $|A_{\perp}|^2$, $|A_{\parallel}|^2$, δ_{\parallel} , δ_{\perp} , and $\delta_{S\perp}$ are extracted with a simultaneous unbinned multidimensional extended maximum likelihood fit to the B_s^0 datasets using seven observables as input: $m_{\mu\mu KK}$, ct , σ_{ct} , $\cos \theta_T$, $\cos \psi_T$, φ_T , and ω_{tag} . The $B_s^0 \rightarrow J/\psi \phi(1020)$ amplitudes are normalized to unity with the constraint $|A_{\parallel}|^2 \equiv 1 - |A_{\perp}|^2 - |A_0|^2$. The likelihood function is composed of probability density functions (PDFs) describing the $B_s^0 \rightarrow J/\psi \phi(1020)$ signal, the combinatorial background, and the background from $B^0 \rightarrow J/\psi K^*(892)^0 \rightarrow \mu^+ \mu^- K^+ \pi^-$, where the pion is misidentified as a kaon (“ B^0 background”). For each component, the PDF is the product of functions that model the distributions of the seven observables of the reconstructed candidates. Correlations between the input observables have been studied in data and simulation and found to have a negligible effect. The $B_s^0 \rightarrow J/\psi \phi(1020)$ differential decay rate model utilized in the fit includes the flavor inference ξ_{tag} and the dilution term \mathcal{D}_{tag} . Unless specified otherwise, all PDF parameters are left free in the final fit. The fit model also includes the angular efficiency and time resolution functions. These functions are computed separately for each main dataset.

The event reconstruction and selection efficiency as a function of ct , $\epsilon(ct)$, is determined from data utilizing the B^0 control data sample, which exhibits a similar topology to the $B_s^0 \rightarrow J/\psi \phi(1020)$ signal. The efficiency is parameterized using Bernstein polynomials to model the ratio

between the observed ct distribution for the signal and the expected distribution convolved with the time resolution. The expected distribution is an exponential characterized by the B^0 lifetime $\tau_{B^0}^{\text{PDG}} = 1.517$ ps [33]. Residual efficiency differences between the control and measurement samples are corrected using simulation. In the fit, each event in the B_s^0 data sample is weighted by $1/\varepsilon(ct)$. Since no dependence of the time resolution on ct is observed in simulation, the ct uncertainty is calibrated for each main dataset in bins of σ_{ct} in a data sample of prompt events obtained by removing the displacement requirement from the MT trigger category. Most of these events consist of prompt $J/\psi \rightarrow \mu^+\mu^-$ decays accompanied by two tracks and are not anticipated to have a substantial lifetime. The long-lived components are properly accounted for. The negative portion of the ct distribution in this sample arises from resolution effects and is used to calibrate σ_{ct} . The ct uncertainty matches the experimental time resolution well, with only a uniform correction of $+1.5$ μm being needed. The calibrated σ_{ct} average value for signal candidates is ≈ 20 μm . The angular efficiency functions $\varepsilon(\Theta)$ are derived from $B_s^0 \rightarrow J/\psi\phi(1020)$ simulated events in which $\Delta\Gamma_s$ is set to zero to disentangle the angular and time components. These simulated samples are corrected to better match the observed data, taking into account the kinematic properties of the final-state particles and the relevant physical parameters. The angular efficiency is modeled using the kernel density estimation (KDE) method [39,40] from the reconstructed and generated angular distributions and is incorporated in the signal PDF as a three-dimensional (3D) histogram. All parameters describing the efficiency and time resolution calibration are fixed in the final fit.

The mass shapes for the signal and the B^0 background are described by Johnson S_U distributions [41], while an exponential distribution is used for the combinatorial background. The ω_{tag} distribution is modeled for each component using KDE distributions, with separate distributions used for events tagged as B_s^0 and \bar{B}_s^0 . For the B^0 and combinatorial backgrounds, the ct component is modeled with one and two exponential distributions, respectively. The angular variables are described with 3D Bernstein polynomials. The PDFs describing σ_{ct} are modeled for each component by the sum of two Gamma distributions, with their parameters fixed in the final fit based on what is obtained from a series of prefits to the signal region $m_{\mu\mu KK} \in [5.28, 5.45]$ and mass sideband region $m_{\mu\mu KK} \in [5.24, 5.28] \cup [5.45, 5.49]$ GeV. The shape of the B^0 background is obtained from simulated $B^0 \rightarrow J/\psi K^*(892)^0$ events (with the decay generated by `EvtGen` using the `EVTSVVHELAMP` model) reconstructed as $B_s^0 \rightarrow J/\psi\phi(1020)$, while its yield is determined from the B_s^0 data sample via a simultaneous fit to the

invariant mass distributions in both the $B_s^0 \rightarrow J/\psi\phi(1020)$ and $B^0 \rightarrow J/\psi K^*(892)^0$ reconstruction hypotheses. The time resolution for the B^0 background is assumed to be the same as for the B_s^0 signal. All parameters related to the B^0 background are fixed in the final fit. The fit model is duplicated for the four main datasets, with the individual log-likelihoods summed to obtain the full log-likelihood.

The fit model is validated through studies on simulated samples and fits to individual data categories. The statistical uncertainties on the POI are determined using the profile-likelihood method, taking into account the presence of event weights. The procedure is cross-checked with the parametric bootstrap method [42], in which 1300 pseudodatasets are generated from the fitted model and refitted with the reference model. The resulting distributions of the POI are used to verify the coverage of the uncertainty estimates and to evaluate the “fit bias,” defined as the difference between the central values of the bootstrap distribution and the reference fit results. This bias is treated as a systematic uncertainty. As an additional cross-check, a set of 400 nonparametric bootstrap pseudodatasets, obtained by sampling events with replacement directly from the data, has also been generated. Considering the associated uncertainties, the results obtained with the profile-likelihood, parametric bootstrap, and nonparametric bootstrap methods are consistent with each other. The measured number of $B_s^0 \rightarrow J/\psi\phi(1020)$ signal events from the fit is $491\,270 \pm 950$, corresponding to an effective number of tagged signal candidates of $N_{B_s^0} P_{\text{tag}} = 27\,500 \pm 100$.

The systematic uncertainties potentially impacting the POI are categorized into two groups. Type-I uncertainties stem from the finite number of events in the simulated samples and from uncertainties related to the parameters of the efficiency and calibration functions. These uncertainties are evaluated by either sampling the function parameters based on their uncertainties or, in the case of nonparametric functions, by resampling the simulated samples. The systematic uncertainties are then quantified as the root-mean-square of the resulting POI distributions. Type-II uncertainties account for potential biases resulting from the assumptions made in the fit model and analysis methods. For each tested assumption, an alternative model choice is selected, and the fit to the data is repeated. A deviation from the reference results is significant if it exceeds 20% of the statistical uncertainty associated with a parameter. In such cases, a double-sided systematic uncertainty of size equal to the deviation is assigned. The fit bias does not fall into either of these two categories. It is evaluated, as discussed above, from the parametric bootstrap distributions and treated as a double-sided systematic uncertainty. The systematic uncertainties are summarized in Table I.

TABLE I. Summary of the systematic and statistical uncertainties. The symbol (\cdots) indicates that no uncertainty is evaluated, as all tested type-II effects are below the threshold to be considered significant. The combined systematic uncertainty is the sum in quadrature of the individual uncertainties.

	ϕ_s (mrad)	$\Delta\Gamma_s$ (ps $^{-1}$)	Γ_s (ps $^{-1}$)	Δm_s (\hbar ps $^{-1}$)	$ \lambda $	$ A_0 ^2$	$ A_\perp ^2$	$ A_S ^2$	δ_\parallel (rad)	δ_\perp (rad)	$\delta_{S\perp}$ (rad)
Statistical uncertainty	22	0.0040	0.0015	0.040	0.014	0.0015	0.0020	0.0034	0.077	0.096	0.16
Fit bias	4	0.0011	0.0002	0.004	0.006	0.0012	0.0022	0.0006	0.015	0.017	0.03
Flavor tagging	8	$<10^{-4}$	0.0010	0.015	0.003	$<10^{-4}$	$<10^{-4}$	0.0012	0.024	0.033	0.06
Angular efficiency	4	0.0002	$<10^{-4}$	0.017	0.013	0.0084	0.0039	0.0001	0.017	0.051	0.02
Time efficiency	<1	0.0014	0.0026	$<10^{-3}$	$<10^{-3}$	0.0004	0.0005	$<10^{-4}$	0.001	0.002	$<10^{-2}$
Time resolution	<1	$<10^{-4}$	$<10^{-4}$	$<10^{-3}$	$<10^{-3}$	$<10^{-4}$	$<10^{-4}$	$<10^{-4}$	$<10^{-3}$	0.001	$<10^{-3}$
Model assumptions	\cdots	0.0015	0.0018	\cdots	\cdots	0.0009	0.0009	\cdots	\cdots	\cdots	\cdots
B^0 background	<1	0.0002	0.0006	$<10^{-3}$	$<10^{-3}$	$<10^{-4}$	$<10^{-4}$	$<10^{-4}$	$<10^{-3}$	$<10^{-3}$	$<10^{-2}$
Λ_b^0 background	\cdots	\cdots	0.0008	\cdots	\cdots	0.0008	0.0006	\cdots	\cdots	\cdots	\cdots
S - P -wave interference	<1	$<10^{-4}$	$<10^{-4}$	$<10^{-3}$	$<10^{-3}$	$<10^{-4}$	$<10^{-4}$	$<10^{-4}$	$<10^{-3}$	$<10^{-3}$	$<10^{-2}$
$P(\sigma_{ct})$ uncertainty	<1	0.0002	0.0003	$<10^{-3}$	$<10^{-3}$	0.0001	0.0001	$<10^{-4}$	$<10^{-3}$	$<10^{-3}$	$<10^{-2}$
Total systematic uncertainty	10	0.0024	0.0034	0.023	0.015	0.0086	0.0047	0.0013	0.033	0.063	0.07

Type-I uncertainties are evaluated for the B^0 background yield, the values of k_{SP} and $\tau_{B^0}^{\text{PDG}}$, and the parameters of the time resolution, time efficiency, and flavor-tagging calibration functions. Similarly, uncertainties arising from the fixed σ_{ct} PDFs in the final fit are also evaluated. Statistical uncertainties associated with the angular efficiency function are estimated using resampling techniques on the $B_s^0 \rightarrow J/\psi\phi(1020)$ simulated events.

Type-II uncertainties are assigned by conducting extensive investigations and cross-verification processes to validate the model assumptions. We explore alternative hypotheses regarding the PDF shapes of the mass, ct , σ_{ct} , ω_{tag} , and angular variable distributions for both the signal and background components. For the prefits, different signal and sideband regions were tried and the $sPlot$ method [43] was used in place of simple sideband subtraction. Additionally, we examine alternative models for the efficiency functions to identify potential sources of bias. The impact of neglecting background from $\Lambda_b^0 \rightarrow J/\psi p K^- \rightarrow \mu^+ \mu^- p K^-$ is assessed by incorporating a dedicated component into the fit model, following an approach similar to the one for the B^0 background, and repeating the fit to the B_s^0 data sample. Various validation studies are carried out on the correction procedure applied to the simulated samples used to evaluate the angular efficiency. The calibration procedure for the OS tagging algorithms is evaluated using results from simulation to correct for differences between $B_s^0 \rightarrow J/\psi\phi(1020)$ and $B^+ \rightarrow J/\psi K^+$ decays. The calibration for the SS tagger already accounts for these differences. We investigate its calibration strategy by removing these corrections, which introduce a significant perturbation of approximately 10% to the calibration parameters, and testing the stability of the physics results in response to these changes. Additionally, possible differences in the calibration between B_s^0/B^+ and \bar{B}_s^0/B^- decays are tested with flavor-

specific calibrations, and no significant impact on the POI is observed.

The fit results, along with the associated statistical and systematic uncertainties, are provided in Table II. The projection of the fit onto each of the seven fitted distributions for the ST trigger category (2018 data) is shown in Figs. 1–3. The results are found to be consistent with SM-based predictions [4,5,44] and the latest world-average values [33]. The weak CPV phase is measured to be $\phi_s = -73 \pm 22(\text{stat}) \pm 10(\text{syst})$ mrad, which is within 1.5 standard deviations of the SM-based prediction. The measured value of $|\lambda|$ is consistent with no direct CPV ($|\lambda| = 1$). These results are comparable in precision to the world's most precise single measurement [20] and supersede the previous results in Ref. [15]. The results are combined with those obtained by CMS at $\sqrt{s} = 8$ TeV [14] using the BLUE method [45,46] to obtain $\phi_s = -75 \pm 23$ mrad and $\Delta\Gamma_s = 0.0778 \pm 0.0046$ ps $^{-1}$,

TABLE II. Measured values and uncertainties of the parameters of interest in the $\Delta\Gamma_s > 0$ region.

Parameter	Fit value	Stat. unc.	Syst. unc.
ϕ_s (mrad)	-73	± 22	± 10
$\Delta\Gamma_s$ (ps $^{-1}$)	0.0761	± 0.0040	± 0.0024
Γ_s (ps $^{-1}$)	0.6613	± 0.0015	± 0.0034
Δm_s (\hbar ps $^{-1}$)	17.757	± 0.040	± 0.023
$ \lambda $	1.011	± 0.014	± 0.015
$ A_0 ^2$	0.5300	± 0.0015	± 0.0086
$ A_\perp ^2$	0.2409	± 0.0020	± 0.0047
$ A_S ^2$	0.0067	$^{+0.0034}_{-0.0027}$	± 0.0013
δ_\parallel (rad)	3.145	± 0.077	± 0.033
δ_\perp (rad)	2.931	± 0.096	± 0.063
$\delta_{S\perp}$ (rad)	0.48	$^{+0.11}_{-0.16}$	± 0.07

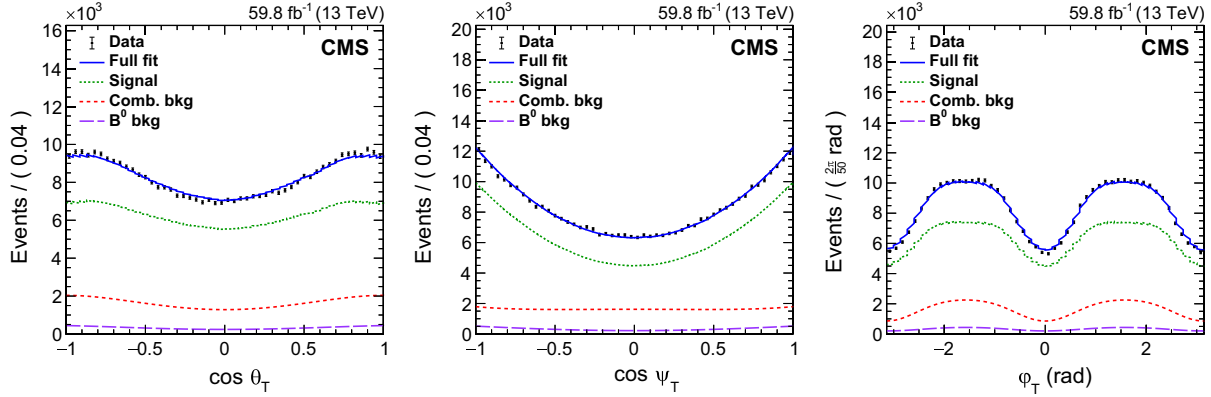


FIG. 3. Angular observable distributions of the selected candidates and fit projection for the ST trigger category (2018 data). The projections of the fitted model are also shown.

which are both compatible with SM-based predictions. The uncertainties include both statistical and systematic components. The full set of combined results is reported in Supplemental Material [38]. Figure 4 shows the two-dimensional ϕ_s versus $\Delta\Gamma_s$ contour at 68% confidence level (CL) for the combined results, alongside the SM-based prediction and the latest results from other LHC experiments. Tabulated results are provided in the HEPData record for this analysis [47]. The combined ϕ_s value exhibits a deviation from zero of 3.2 standard deviations, providing the first evidence for mixing-induced CPV in $B_s^0 \rightarrow J/\psi\phi(1020)$ decays.

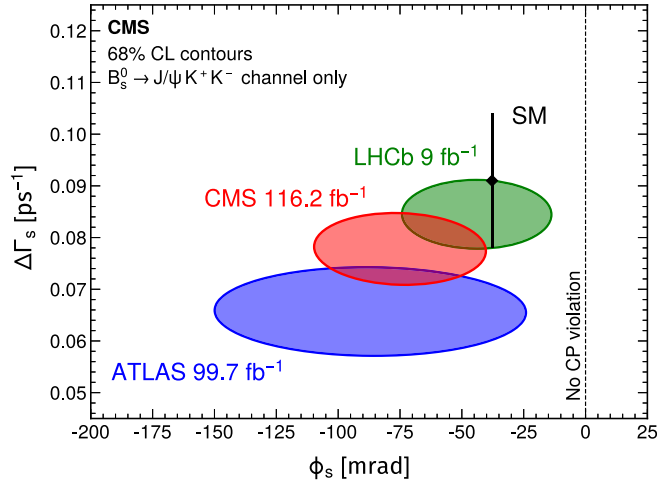


FIG. 4. The two-dimensional 68% CL contours in the ϕ_s - $\Delta\Gamma_s$ plane for the combined CMS (red), ATLAS (blue) [26], and LHCb (green) [20] results. Results refer only to $B_s^0 \rightarrow J/\psi K^+ K^-$ measurements in the $\Delta\Gamma_s > 0$ region. The contours account for both statistical and systematic uncertainties. The SM prediction neglects possible contributions from higher-order penguin diagrams and is represented by the thin black band, with the central value indicated by the black diamond [4,5,44].

Acknowledgments—We congratulate our colleagues in the CERN accelerator departments for the excellent performance of the LHC and thank the technical and administrative staffs at CERN and at other CMS institutes for their contributions to the success of the CMS effort. In addition, we gratefully acknowledge the computing centers and personnel of the Worldwide LHC Computing Grid and other centers for delivering so effectively the computing infrastructure essential to our analyses. Finally, we acknowledge the enduring support for the construction and operation of the LHC, the CMS detector, and the supporting computing infrastructure provided by the following funding agencies: SC (Armenia), BMBWF and FWF (Austria); FNRS and FWO (Belgium); CNPq, CAPES, FAPERJ, FAPERGS, and FAPESP (Brazil); MES and BNSF (Bulgaria); CERN; CAS, MoST, and NSFC (China); Minciencias (Colombia); MSES and CSF (Croatia); RIF (Cyprus); SENESCYT (Ecuador); ERC PRG, RVTT3, and MoER TK202 (Estonia); Academy of Finland, MEC, and HIP (Finland); CEA and CNRS/IN2P3 (France); SRNSF (Georgia); BMBF, DFG, and HGF (Germany); GSRI (Greece); NKFIH (Hungary); DAE and DST (India); IPM (Iran); SFI (Ireland); INFN (Italy); MSIP and NRF (Republic of Korea); MES (Latvia); LMTLT (Lithuania); MOE and UM (Malaysia); BUAP, CINVESTAV, CONACYT, LNS, SEP, and UASLP-FAI (Mexico); MOS (Montenegro); MBIE (New Zealand); PAEC (Pakistan); MES and NSC (Poland); FCT (Portugal); MESTD (Serbia); MCIN/AEI and PCTI (Spain); MOSTR (Sri Lanka); Swiss Funding Agencies (Switzerland); MST (Taipei); MHESI and NSTDA (Thailand); TUBITAK and TENMAK (Turkey); NASU (Ukraine); STFC (United Kingdom); DOE and NSF (USA).

Data availability—Release and preservation of data used by the CMS Collaboration as the basis for publications is guided by the CMS data preservation, reuse, and open access policy [48].

- [1] N. Cabibbo, Unitary symmetry and leptonic decays, *Phys. Rev. Lett.* **10**, 531 (1963).
- [2] M. Kobayashi and T. Maskawa, CP violation in the renormalizable theory of weak interaction, *Prog. Theor. Phys.* **49**, 652 (1973).
- [3] M. Z. Barel, K. De Bruyn, R. Fleischer, and E. Malami, In pursuit of new physics with $B^0 \rightarrow J/\psi K^0$ and $B_s^0 \rightarrow J/\psi \phi(1020)$ decays at the high-precision frontier, *J. Phys. G* **48**, 065002 (2021).
- [4] J. Charles, O. Deschamps, S. Descotes-Genon, R. Itoh, H. Lacker, A. Menzel, S. Monteil, V. Niess, J. Ocariz, J. Orloff, S. T'Jampens, V. Tisserand, and K. Trabelsi (CKMfitter Collaboration), Predictions of selected flavour observables within the standard model, *Phys. Rev. D* **84**, 033005 (2011), updated with Summer 23 results: http://ckmfitter.in2p3.fr/www/results/plots_summer23/ckm_res_summer23.html.
- [5] M. Bona *et al.* (UTfit Collaboration), New UTfit analysis of the unitarity triangle in the Cabibbo–Kobayashi–Maskawa scheme, *Rend. Lincei Sci. Fis. Nat.* **34**, 37 (2023).
- [6] A. Abulencia *et al.* (CDF Collaboration), Observation of $B_s^0 - \bar{B}_s^0$ oscillations, *Phys. Rev. Lett.* **97**, 242003 (2006).
- [7] C.-W. Chiang, A. Datta, M. Duraisamy, D. London, M. Nagashima, and A. Szykman, New physics in $B_s^0 \rightarrow J/\psi \phi(1020)$: A general analysis, *J. High Energy Phys.* **04** (2010) 031.
- [8] M. Artuso, G. Borissov, and A. Lenz, CP violation in the B_s^0 system, *Rev. Mod. Phys.* **88**, 045002 (2016); **91**, 049901(E) (2019).
- [9] V. M. Abazov *et al.* (D0 Collaboration), Measurement of B_s^0 mixing parameters from the flavor-tagged decay $B_s^0 \rightarrow J/\psi \phi(1020)$, *Phys. Rev. Lett.* **101**, 241801 (2008).
- [10] V. M. Abazov *et al.* (D0 Collaboration), Measurement of the CP -violating phase $\phi_s^{J/\psi \phi}$ using the flavor-tagged decay $B_s^0 \rightarrow J/\psi \phi(1020)$ in 8 fb^{-1} of $p\bar{p}$ collisions, *Phys. Rev. D* **85**, 032006 (2012).
- [11] T. Aaltonen *et al.* (CDF Collaboration), First flavor-tagged determination of bounds on mixing-induced CP violation in $B_s^0 \rightarrow J/\psi \phi(1020)$ decays, *Phys. Rev. Lett.* **100**, 161802 (2008).
- [12] T. Aaltonen *et al.* (CDF Collaboration), Measurement of the CP -violating phase $\beta_s^{J/\psi \phi}$ in $B_s^0 \rightarrow J/\psi \phi(1020)$ decays with the CDF II detector, *Phys. Rev. D* **85**, 072002 (2012).
- [13] T. Aaltonen *et al.* (CDF Collaboration), Measurement of the bottom-strange meson mixing phase in the full CDF data set, *Phys. Rev. Lett.* **109**, 171802 (2012).
- [14] CMS Collaboration, Measurement of the CP -violating weak phase ϕ_s and the decay width difference $\Delta\Gamma_s$ using the $B_s^0 \rightarrow J/\psi \phi(1020)$ decay channel in pp collisions at $\sqrt{s} = 8 \text{ TeV}$, *Phys. Lett. B* **757**, 97 (2016).
- [15] CMS Collaboration, Measurement of the CP -violating phase ϕ_s in the $B_s^0 \rightarrow J/\psi \phi(1020) \rightarrow \mu^+ \mu^- K^+ K^-$ channel in proton-proton collisions at $\sqrt{s} = 13 \text{ TeV}$, *Phys. Lett. B* **816**, 136188 (2021).
- [16] LHCb Collaboration, Measurement of the CP -violating phase ϕ_s in $\bar{B}_s^0 \rightarrow J/\psi \pi^+ \pi^-$ decays, *Phys. Lett. B* **713**, 378 (2012).
- [17] LHCb Collaboration, Measurement of CP violation and the B_s^0 meson decay width difference with $B_s^0 \rightarrow J/\psi K^+ K^-$ and $B_s^0 \rightarrow J/\psi \pi^+ \pi^-$ decays, *Phys. Rev. D* **87**, 112010 (2013).
- [18] LHCb Collaboration, Measurement of the CP -violating phase ϕ_s in $\bar{B}_s^0 \rightarrow J/\psi \pi^+ \pi^-$ decays, *Phys. Lett. B* **736**, 186 (2014).
- [19] LHCb Collaboration, Precision measurement of CP violation in $B_s^0 \rightarrow J/\psi K^+ K^-$ decays, *Phys. Rev. Lett.* **114**, 041801 (2015).
- [20] LHCb Collaboration, Improved measurement of CP violation parameters in $B_s^0 \rightarrow J/\psi K^+ K^-$ decays in the vicinity of the $\phi(1020)$, *Phys. Rev. Lett.* **132**, 051802 (2024).
- [21] LHCb Collaboration, Measurement of the CP -violating phase ϕ_s in $\bar{B}_s^0 \rightarrow D_s^+ D_s^-$ decays, *Phys. Rev. Lett.* **113**, 211801 (2014).
- [22] LHCb Collaboration, First study of the CP -violating phase and decay-width difference in $B_s^0 \rightarrow \psi(2S)\phi$, *Phys. Lett. B* **762**, 253 (2016).
- [23] ATLAS Collaboration, Time-dependent angular analysis of the decay $B_s^0 \rightarrow J/\psi \phi(1020)$ and extraction of $\Delta\Gamma_s$ and the CP -violating weak phase ϕ_s by ATLAS, *J. High Energy Phys.* **12** (2012) 072.
- [24] ATLAS Collaboration, Flavor tagged time-dependent angular analysis of the $B_s^0 \rightarrow J/\psi \phi(1020)$ decay and extraction of $\Delta\Gamma_s$ and the weak phase ϕ_s in ATLAS, *Phys. Rev. D* **90**, 052007 (2014).
- [25] ATLAS Collaboration, Measurement of the CP -violating phase ϕ_s and the B_s^0 meson decay width difference with $B_s^0 \rightarrow J/\psi \phi(1020)$ decays in ATLAS, *J. High Energy Phys.* **12** (2016) 072.
- [26] ATLAS Collaboration, Measurement of the CP -violating phase ϕ_s in $B_s^0 \rightarrow J/\psi \phi(1020)$ decays in ATLAS at 13 TeV, *Eur. Phys. J. C* **81**, 342 (2021).
- [27] CMS Collaboration, The CMS experiment at the CERN LHC, *J. Instrum.* **3**, S08004 (2008).
- [28] CMS Collaboration, Development of the CMS detector for the CERN LHC Run 3, *J. Instrum.* **19**, P05064 (2024).
- [29] CMS Collaboration, Precision luminosity measurement in proton-proton collisions at $\sqrt{s} = 13 \text{ TeV}$ in 2015 and 2016 at CMS, *Eur. Phys. J. C* **81**, 800 (2021).
- [30] CMS Collaboration, CMS luminosity measurement for the 2017 data-taking period at $\sqrt{s} = 13 \text{ TeV}$, CMS Physics Analysis Summary Report No. CMS-PAS-LUM-17-004, 2018, <https://cds.cern.ch/record/2621960>.
- [31] CMS Collaboration, CMS luminosity measurement for the 2018 data-taking period at $\sqrt{s} = 13 \text{ TeV}$, CMS Physics Analysis Summary Report No. CMS-PAS-LUM-18-002, 2019, <https://cds.cern.ch/record/2676164>.
- [32] A. S. Dighe, I. Dunietz, and R. Fleischer, Extracting CKM phases and $B_s^0 - \bar{B}_s^0$ mixing parameters from angular distributions of non-leptonic B decays, *Eur. Phys. J. C* **6**, 647 (1999).
- [33] S. Navas *et al.* (Particle Data Group), Review of particle physics, *Phys. Rev. D* **2024**, 030001 (2024).
- [34] G. C. Branco, L. Lavoura, and J. P. Silva, *CP Violation, International Series of Monographs on Physics* Vol. 103 (Clarendon Press, Oxford, United Kingdom, 1999).

- [35] S. M. Flatté, On the nature of 0^+ mesons, *Phys. Lett.* **63B**, 228 (1976).
- [36] LHCb Collaboration, Determination of the sign of the decay width difference in the B_s^0 system, *Phys. Rev. Lett.* **108**, 241801 (2012).
- [37] CMS Collaboration, The CMS trigger system, *J. Instrum.* **12**, P01020 (2017).
- [38] See Supplemental Material at <http://link.aps.org/supplemental/10.1103/ctqx-vxrj> for additional figures and tables.
- [39] M. Rosenblatt, Remarks on some nonparametric estimates of a density function, *Ann. Math. Stat.* **27**, 832 (1956).
- [40] E. Parzen, On estimation of a probability density function and mode, *Ann. Math. Stat.* **33**, 1065 (1962).
- [41] N. L. Johnson, Systems of frequency curves generated by methods of translation, *Biometrika* **36**, 149 (1949).
- [42] B. Efron and R. J. Tibshirani, *An Introduction to the Bootstrap*, Monographs on Statistics and Applied Probability (Chapman & Hall/CRC, Boca Raton, Florida, USA, 1993).
- [43] M. Pivk and F. R. Le Diberder, $sPlot$: A statistical tool to unfold data distributions, *Nucl. Instrum. Methods Phys. Res., Sect. A* **555**, 356 (2005).
- [44] A. Lenz and G. Tetlalmatzi-Xolocotzi, Model-independent bounds on new physics effects in non-leptonic tree-level decays of B -mesons, *J. High Energy Phys.* **07** (2020) 177.
- [45] L. Lyons, D. Gibaut, and P. Clifford, How to combine correlated estimates of a single physical quantity, *Nucl. Instrum. Methods Phys. Res., Sect. A* **270**, 110 (1988).
- [46] A. Valassi, Combining correlated measurements of several different physical quantities, *Nucl. Instrum. Methods Phys. Res., Sect. A* **500**, 391 (2003).
- [47] HEPData record for this analysis, [10.17182/hepdata.156384](https://hepdata.net/record/10.17182/hepdata.156384) (2024).
- [48] CMS data availability statement, [10.7483/OPENDATA.CMS.IBNU.8V1W](https://cds.cern.ch/record/10.7483/OPENDATA.CMS.IBNU.8V1W).
- [49] CMS Collaboration, Performance of the CMS Level-1 trigger in proton-proton collisions at $\sqrt{s} = 13$ TeV, *J. Instrum.* **15**, P10017 (2020).
- [50] CMS Collaboration, Electron and photon reconstruction and identification with the CMS experiment at the CERN LHC, *J. Instrum.* **16**, P05014 (2021).
- [51] CMS Collaboration, Performance of the CMS muon detector and muon reconstruction with proton-proton collisions at $\sqrt{s} = 13$ TeV, *J. Instrum.* **13**, P06015 (2018).
- [52] CMS Collaboration, Description and performance of track and primary-vertex reconstruction with the CMS tracker, *J. Instrum.* **9**, P10009 (2014).
- [53] CMS Collaboration, Particle-flow reconstruction and global event description with the CMS detector, *J. Instrum.* **12**, P10003 (2017).
- [54] T. Sjöstrand, S. Ask, J. R. Christiansen, R. Corke, N. Desai, P. Ilten, S. Mrenna, S. Prestel, C. O. Rasmussen, and P. Z. Skands, An introduction to PYTHIA 8.2, *Comput. Phys. Commun.* **191**, 159 (2015).
- [55] CMS Collaboration, Extraction and validation of a new set of CMS PYTHIA8 tunes from underlying-event measurements, *Eur. Phys. J. C* **80**, 4 (2020).
- [56] R. D. Ball *et al.* (NNPDF Collaboration), Parton distributions from high-precision collider data, *Eur. Phys. J. C* **77**, 663 (2017).
- [57] D. J. Lange, The EvtGen particle decay simulation package, *Nucl. Instrum. Methods Phys. Res., Sect. A* **462**, 152 (2001).
- [58] E. Barberio and Z. Waş, Photos—A universal Monte Carlo for QED radiative corrections: Version 2.0, *Comput. Phys. Commun.* **79**, 291 (1994).
- [59] S. Agostinelli *et al.* (Geant4 Collaboration), Geant4—A simulation toolkit, *Nucl. Instrum. Methods Phys. Res., Sect. A* **506**, 250 (2003).
- [60] R. Frühwirth, Application of Kalman filtering to track and vertex fitting, *Nucl. Instrum. Methods Phys. Res., Sect. A* **262**, 444 (1987).
- [61] M. Zaheer, S. Kottur, S. Ravanbakhsh, B. Poczós, R. Salakhutdinov, and A. Smola, Deep sets, [arXiv:1703.06114](https://arxiv.org/abs/1703.06114).
- [62] CMS Collaboration, Identification of heavy-flavour jets with the CMS detector in pp collisions at 13 TeV, *J. Instrum.* **13**, P05011 (2018).
- [63] D.-A. Clevert, T. Unterthiner, and S. Hochreiter, Fast and accurate deep network learning by Exponential Linear Units (ELUs), [arXiv:1511.07289](https://arxiv.org/abs/1511.07289).
- [64] J. Platt, *Probabilities for SV Machines* (The MIT Press, Cambridge, MA, 2000), Chap. 5, p. 61.
- [65] D. Kingma and J. Ba, Adam: A method for stochastic optimization, in *Proceedings of International Conference on Learning Representations* (2014), [arXiv:1412.6980](https://arxiv.org/abs/1412.6980).

End Matter

Appendix A: The CMS detector, simulated samples, and event reconstruction—The CMS apparatus is a multipurpose, nearly hermetic detector, designed to trigger on [37,49] and identify electrons, muons, photons, and hadrons [50–52]. A global event description algorithm [53] aims to reconstruct all individual particles in an event, combining information provided by the all-silicon tracker and by the crystal electromagnetic and brass-scintillator hadron calorimeters, operating inside a 3.8 T superconducting solenoid, with data from the gas-ionization muon detectors interleaved with the layers of the flux-return yoke outside the solenoid. Simulated events are employed to determine the angular efficiency

and to train the various machine-learning models. These samples are generated with the software described in Refs. [54–59] and validated via comparison with background-subtracted data in several control distributions.

To improve the purity of the signal, additional requirements are imposed on events selected by the trigger system. Muons and kaons must have pseudorapidity $|\eta| < 2.4$ and $|\eta| < 2.5$, respectively. For the MT (ST) trigger category, muons are required to have transverse momentum $p_T > 3.5(4.0)$ GeV, while tracks are required to have $p_T > 1.15(0.90)$ GeV. The opposite-charge muons forming the J/ψ candidate are then constrained to a common

vertex, obtained via a Kalman fit [60], with an invariant mass within 150 MeV of the world-average mass of the J/ψ meson [33]. The $\phi(1020)$ meson candidates are retained only if their invariant mass, assuming both oppositely charged particles to be kaons, lies within 10 MeV of the world-average mass of the $\phi(1020)$ meson [33]. Finally, the J/ψ and $\phi(1020)$ meson candidates are combined to create B_s^0 meson candidates through a kinematic fitting process involving the four tracks, where the dimuon mass is constrained to the world-average J/ψ meson mass [33]. The B_s^0 meson candidates are accepted if their $p_T > 9.5$ GeV, their invariant mass is in the 5.24–5.49 GeV range, and the vertex fit χ^2 probability exceeds 2%. The primary vertex (PV) is chosen as the vertex closest to the line passing through the B_s^0 decay vertex and parallel to its momentum. The ct is measured as $ct = cm_{B_s^0}^{\text{PDG}} \vec{L}_{xy} \cdot \vec{p}_T / p_T^2$, where $m_{B_s^0}^{\text{PDG}}$ is the world-average B_s^0 mass [33] and \vec{L}_{xy} is the vector from the PV to the B_s^0 vertex in the transverse plane. The ct uncertainty σ_{ct} is obtained by propagating the uncertainties in L_{xy} and p_T of the B_s^0 meson candidate to ct . It is required that $ct \geq 60(100)$ μm for the MT (ST) trigger category, with $\sigma_{ct} < 50$ μm . Additionally, events in the ST trigger category need to satisfy $ct/\sigma_{ct} > 3$. In approximately 2% of the events, multiple B_s^0 meson candidates are reconstructed, and in these cases the candidate with the highest vertex-fit probability is chosen.

Appendix B: Flavor tagging—The OS muon and OS electron taggers follow the same strategy. They search for semileptonic $b \rightarrow \ell^- + X$ decays of the OS b quark, using the lepton charge as the tagging variable and subsequently employing DNNs to estimate ω_{tag} . For each event, we search for a candidate OS lepton consistent with being produced by the OS b hadron. To reduce contamination from background sources, loose kinematic requirements are imposed on the candidates, and DNN discriminators are used to reduce contributions from hadrons and photons misreconstructed as muons and electrons, respectively. To avoid overlaps, an OS electron is searched only if no OS muon is found. In both algorithms, conditions are introduced to separate the OS lepton from the B_s^0 meson candidate. An ensemble of DNNs is used to discriminate the right- and wrong-tag leptons, as well as to estimate the event mistag probability. The DNNs have been developed using simulated $B_s^0 \rightarrow J/\psi\phi(1020)$ events and calibrated with self-tagging $B^+ \rightarrow J/\psi K^+$ data samples, as described below. The input features of the lepton-tagging DNNs consist of variables extracted from the kinematic properties of the lepton candidate and the surrounding activity. The structure of all DNN models has been optimized to maximize the tagging power. The architecture is purposefully designed so that its output

score “ s_{DNN} ” corresponds directly to the probability of correctly tagging an event.

The OS jet tagger is based on DNNs, referred to collectively as “DeepJetCharge” (DJC), derived from the Deep Sets architecture [61] and exploits charge asymmetries in OS b jets to predict the probability of being produced by b versus \bar{b} quarks. The resulting probability serves as the basis for determining both ξ_{tag} and ω_{tag} . An OS jet candidate is selected if it passes loose kinematic requirements, does not contain tracks from the signal B_s^0 , the probability P_b of originating from a bottom or anti-bottom quark, as estimated by DeepJet [62] exceeds 20%, and contains at least two tracks from the PV. To ensure the OS algorithms are orthogonal to each other, an OS jet is searched for only if no OS muon or OS electron is found. Features used by DJC include p_T and η of the B_s^0 meson, p_T , η , and P_b of the jet, and the angular distances $\Delta R \equiv \sqrt{(\Delta\eta)^2 + (\Delta\phi)^2}$ and $\Delta\phi$ between the direction of the jet and that of the B_s^0 . Features from at most 15 charged particles (ordered by the longitudinal impact parameter relative to the PV, d_z) are also included: charge, p_T , η , ΔR , and $\Delta\phi$ relative to the B_s^0 momentum, impact parameters with respect to the PV, and their uncertainties. In addition to the jet constituents, other tracks in a $\Delta R < 0.5$ cone around the jet axis are used to recover tracks not found by the jet reconstruction. The DJC is trained on simulated $B_s^0 \rightarrow J/\psi\phi(1020)$ events of the ST trigger category and its structure is composed of four blocks. First, three dense layers act on every input feature except track charge, making this block explicitly flavor invariant. Then, the charge information is added and two more dense layers are executed. Subsequently, all the hidden features are summed across all tracks, flattening the track vector to a single dimension. Finally, four interlaced dense and drop-out layers convert the feature vector to a probability, which is the model output. All dense layers use an exponential linear unit activation function [63]. To preserve symmetry between the two classes, that is b and \bar{b} jets, the algorithm is constructed as flavor invariant, that is the probabilities for the b hypothesis are identical to those of the \bar{b} hypothesis when inverting all the charges. This is achieved by explicitly symmetrizing the output as $s_{\text{DJC}}(x) = [s_{\text{DJC}}(x) + (1 - s_{\text{DJC}}(\bar{x}))]/2$, where x is the model input and \bar{x} is the input with all the track charges reversed. The output of DJC coincides with the probability of the OS jet being produced by a bottom quark, which can be straightforwardly used to perform the tagging inference and ω_{tag} estimation.

The SS tagger, referred to as “DeepSameSide” (DSS), exploits the correlation between the quark content of the B_s^0 meson at production time and the charges of the fragmentation particles surrounding it. Consequently, it is independent of the OS tag, is not diluted by mixing in the other b quark, and does not depend on the presence of its decay

products from the other b quark, such as leptons or jets, within the acceptance of the CMS detector. The architecture of DSS is modeled on that of DJC (including output symmetrization), exploiting the features from the B_s^0 meson candidate and all the tracks, other than its constituents, in a $\Delta R = 0.8$ cone around its direction (care is taken to avoid geometrical overlap with the OS methods). Up to 20 tracks, ordered by d_z , are considered; in contrast to DJC, no jet features are used. The DSS is trained on a sample of B_s^0 and B^+ simulated events to compute the probability of having a bottom quark at production time. The B^+ events are used to render the algorithm invariant for $B_s^0 \leftrightarrow B^-$ and $\bar{B}_s^0 \leftrightarrow B^+$ transformation and allow the calibration in data with $B^+ \rightarrow J/\psi K^+$ decays. The DSS exploits the charge of the particles produced in the hadronization for the discrimination, which depends on the light quark in the meson. The DSS is trained to produce the probability of an initial signal B_s^0 meson, from which the tagging inference and ω_{tag} estimation can be then performed.

The event mistag probability, as estimated by the tagging algorithms, undergoes calibration utilizing a self-tagging data sample of $B^+ \rightarrow J/\psi K^+$ events, where the kaon's charge corresponds to the B^+ meson flavor. The calibration procedure is executed separately for each dataset, by comparing the measured mistag fraction (ω_{meas}) with the ω_{tag} predicted by the taggers. The B^+ events are divided into bins in ω_{tag} , and, within each bin, the count of right- and wrong-tag events is computed independently on the $J/\psi K^+$ invariant mass distribution to derive the corresponding ω_{meas} value. The $(\omega_{\text{tag}}, \omega_{\text{meas}})$ pairs are then used to refine the DNNs' predictions through the Platt scaling method [64]. This method fits a linear function to the model's output before the final sigmoid layer, effectively calibrating the predicted probabilities to the measured outcomes. In the case of the OS lepton taggers, both parameters of the linear function are left free to float, while for the OS jet and SS tagger, the constant term is set to zero to preserve symmetry between the two flavor hypotheses. The calibration of DSS is further corrected to account for potential differences between B_s^0 and B^+ mesons by using

TABLE III. Calibrated flavor-tagging performance as measured in the B_s^0 data sample in the various mutually exclusive categories. The effective dilution $\mathcal{D}_{\text{tag,eff}}^2$ is obtained from the measured tagging efficiency ϵ_{tag} and tagging power P_{tag} . The uncertainties are statistical only.

Category	$\epsilon_{\text{tag}}(\%)$	$\mathcal{D}_{\text{tag,eff}}^2$	$P_{\text{tag}}(\%)$
Only OS muon	6.07 ± 0.05	0.212	1.29 ± 0.07
Only OS electron	2.72 ± 0.02	0.079	0.214 ± 0.004
Only OS jet	5.16 ± 0.03	0.045	0.235 ± 0.003
Only SS	33.12 ± 0.07	0.080	2.64 ± 0.01
SS + OS muon	0.62 ± 0.01	0.202	0.125 ± 0.003
SS + OS electron	2.77 ± 0.02	0.150	0.416 ± 0.005
SS + OS jet	5.40 ± 0.03	0.124	0.671 ± 0.006
Combined	55.9 ± 0.1	0.100	5.59 ± 0.02

the calibrations obtained in simulated $B_s^0 \rightarrow J/\psi \phi(1020)$ and $B^+ \rightarrow J/\psi K^+$ events. The size of this correction is found to be of the order of 10%. For the OS jet and SS tagger, events with $\omega_{\text{tag}} > 0.48$ and $\omega_{\text{tag}} > 0.46$, respectively, are classified as untagged. These events contribute minimally to the performance, and their removal enhances the calibration reliability.

All tagging DNNs are developed in simulated events and employ the cross-entropy loss function combined with the Adam optimizer [65]. Input features are preprocessed so that the mean and variance for each of the input variables are, respectively, zero and one. The four tracks forming the B_s^0 meson candidate are explicitly excluded from consideration by the taggers and precautions are taken to reduce the effect of multiple collisions in the same or neighboring bunch crossings.

The combined performance of the tagging framework yields a tagging power of $P_{\text{tag}} = (5.59 \pm 0.02)\%$. The tagging efficiency, tagging power, and effective dilution for each exclusive tagging category are presented in Table III.

A. Hayrapetyan,¹ A. Tumasyan,^{1,b} W. Adam,² J. W. Andrejkovic,² L. Benato,² T. Bergauer,² S. Chatterjee,² K. Damanakis,² M. Dragicevic,² P. S. Hussain,² M. Jeitler,^{2,c} N. Krammer,² A. Li,² D. Liko,² I. Mikulec,² J. Schieck,^{2,c} R. Schöfbeck,^{2,c} D. Schwarz,² M. Sonawane,² W. Waltenberger,² C.-E. Wulz,^{2,c} T. Janssen,³ T. Van Laer,³ P. Van Mechelen,³ N. Breugelmans,⁴ J. D'Hondt,⁴ S. Dansana,⁴ A. De Moor,⁴ M. Delcourt,⁴ F. Heyen,⁴ S. Lowette,⁴ I. Makarenko,⁴ D. Müller,⁴ S. Tavernier,⁴ M. Tytgat,^{4,d} G. P. Van Onsem,⁴ S. Van Putte,⁴ D. Vannerom,⁴ B. Bilin,⁵ B. Clerbaux,⁵ A. K. Das,⁵ I. De Bruyn,⁵ G. De Lentdecker,⁵ H. Evard,⁵ L. Favart,⁵ P. Giannelis,⁵ J. Jaramillo,⁵ A. Khalilzadeh,⁵ F. A. Khan,⁵ K. Lee,⁵ A. Malara,⁵ S. Paredes,⁵ M. A. Shahzad,⁵ L. Thomas,⁵ M. Vanden Bemden,⁵ C. Vander Velde,⁵ P. Vanlaer,⁵ M. De Coen,⁶ D. Dobur,⁶ G. Gokbulut,⁶ Y. Hong,⁶ J. Knolle,⁶ L. Lambrecht,⁶ D. Marckx,⁶ K. Mota Amarilo,⁶ K. Skovpen,⁶

N. Van Den Bossche⁶, J. van der Linden⁶, L. Wezenbeek⁶, A. Benecke⁷, A. Bethani⁷, G. Bruno⁷, C. Caputo⁷, J. De Favereau De Jeneret⁷, C. Delaere⁷, I. S. Donertas⁷, A. Giammanco⁷, A. O. Guzel⁷, Sa. Jain⁷, V. Lemaître⁷, J. Lidrych⁷, P. Mastrapasqua⁷, T. T. Tran⁷, G. A. Alves⁸, E. Coelho⁸, G. Correia Silva⁸, C. Hensel⁸, T. Menezes De Oliveira⁸, C. Mora Herrera^{8,e}, P. Rebello Teles⁸, M. Soeiro⁸, A. Vilela Pereira^{8,e}, W. L. Aldá Júnior⁹, M. Barroso Ferreira Filho⁹, H. Brandao Malbouisson⁹, W. Carvalho⁹, J. Chinellato^{9,f}, E. M. Da Costa⁹, G. G. Da Silveira^{9,g}, D. De Jesus Damiao⁹, S. Fonseca De Souza⁹, R. Gomes De Souza⁹, T. Laux Kuhn^{9,g}, M. Macedo⁹, J. Martins⁹, L. Mundim⁹, H. Nogima⁹, J. P. Pinheiro⁹, A. Santoro⁹, A. Sznajder⁹, M. Thiel⁹, C. A. Bernardes^{10,g}, L. Calligaris¹⁰, T. R. Fernandez Perez Tomei¹⁰, E. M. Gregores¹⁰, I. Maietto Silverio¹⁰, P. G. Mercadante¹⁰, S. F. Novaes¹⁰, B. Orzari¹⁰, Sandra S. Padula¹⁰, A. Aleksandrov¹¹, G. Antchev¹¹, R. Hadjiiska¹¹, P. Iaydjiev¹¹, M. Misheva¹¹, M. Shopova¹¹, G. Sultanov¹¹, A. Dimitrov¹², L. Litov¹², B. Pavlov¹², P. Petkov¹², A. Petrov¹², E. Shumka¹², S. Keshri¹³, D. Laroze¹³, S. Thakur¹³, T. Cheng¹⁴, T. Javaid¹⁴, L. Yuan¹⁴, Z. Hu¹⁵, Z. Liang¹⁵, J. Liu¹⁵, G. M. Chen^{16,h}, H. S. Chen^{16,h}, M. Chen^{16,h}, F. Iemmi¹⁶, C. H. Jiang¹⁶, A. Kapoor^{16,i}, H. Liao¹⁶, Z.-A. Liu^{16,h}, R. Sharma^{16,j}, J. N. Song^{16,h}, J. Tao¹⁶, C. Wang^{16,h}, J. Wang¹⁶, Z. Wang^{16,h}, H. Zhang¹⁶, J. Zhao¹⁶, A. Agapitos¹⁷, Y. Ban¹⁷, A. Carvalho Antunes De Oliveira¹⁷, S. Deng¹⁷, B. Guo¹⁷, C. Jiang¹⁷, A. Levin¹⁷, C. Li¹⁷, Q. Li¹⁷, Y. Mao¹⁷, S. Qian¹⁷, S. J. Qian¹⁷, X. Qin¹⁷, X. Sun¹⁷, D. Wang¹⁷, H. Yang¹⁷, L. Zhang¹⁷, Y. Zhao¹⁷, C. Zhou¹⁷, S. Yang¹⁸, Z. You¹⁹, K. Jaffel²⁰, N. Lu²⁰, G. Bauer^{21,k}, B. Li^{21,l}, K. Yi^{21,m}, J. Zhang²¹, Y. Li²², Z. Lin²³, C. Lu²³, M. Xiao²³, C. Avila²⁴, D. A. Barbosa Trujillo²⁴, A. Cabrera²⁴, C. Florez²⁴, J. Fraga²⁴, J. A. Reyes Vega²⁴, F. Ramirez²⁵, C. Rendón²⁵, M. Rodriguez²⁵, A. A. Ruales Barbosa²⁵, J. D. Ruiz Alvarez²⁵, D. Giljanovic²⁶, N. Godinovic²⁶, D. Lelas²⁶, A. Sculac²⁶, M. Kovac²⁷, A. Petkovic²⁷, T. Sculac²⁷, P. Bargassa²⁸, V. Brigljevic²⁸, B. K. Chitroda²⁸, D. Ferencek²⁸, K. Jakovcic²⁸, A. Starodumov^{28,n}, T. Susa²⁸, A. Attikis²⁹, K. Christoforou²⁹, A. Hadjiagapiou²⁹, C. Leonidou²⁹, J. Mousa²⁹, C. Nicolaou²⁹, L. Paizanos²⁹, F. Ptochos²⁹, P. A. Razis²⁹, H. Rykaczewski²⁹, H. Saka²⁹, A. Stepennov²⁹, M. Finger³⁰, M. Finger Jr.³⁰, A. Kveton³⁰, E. Ayala³¹, E. Carrera Jarrin³², B. El-mahdy³³, S. Khalil^{33,o}, E. Salama^{33,p,q}, M. Abdullah Al-Mashad³⁴, M. A. Mahmoud³⁴, K. Ehataht³⁵, M. Kadastik³⁵, T. Lange³⁵, S. Nandan³⁵, C. Nielsen³⁵, J. Pata³⁵, M. Raidal³⁵, L. Tani³⁵, C. Veelken³⁵, H. Kirschenmann³⁶, K. Osterberg³⁶, M. Voutilainen³⁶, S. Bharthuar³⁷, N. Bin Norjoharuddeen³⁷, E. Brücken³⁷, F. Garcia³⁷, P. Inkaew³⁷, K. T. S. Kallonen³⁷, T. Lampén³⁷, K. Lassila-Perini³⁷, S. Lehti³⁷, T. Lindén³⁷, M. Myllymäki³⁷, M. m. Rantanen³⁷, H. Siikonen³⁷, J. Tuominiemi³⁷, P. Luukka³⁸, H. Petrow³⁸, M. Besancon³⁹, F. Couderc³⁹, M. Dejardin³⁹, D. Denegri³⁹, J. L. Faure³⁹, F. Ferri³⁹, S. Ganjour³⁹, P. Gras³⁹, G. Hamel de Monchenault³⁹, M. Kumar³⁹, V. Lohezic³⁹, J. Malcles³⁹, F. Orlandi³⁹, L. Portales³⁹, A. Rosowsky³⁹, M. Ö. Sahin³⁹, A. Savoy-Navarro^{39,r}, P. Simkina³⁹, M. Titov³⁹, M. Tornago³⁹, F. Beaudette⁴⁰, G. Boldrini⁴⁰, P. Busson⁴⁰, A. Cappati⁴⁰, C. Charlot⁴⁰, M. Chiusi⁴⁰, T. D. Cuisset⁴⁰, F. Damas⁴⁰, O. Davignon⁴⁰, A. De Wit⁴⁰, I. T. Ehle⁴⁰, B. A. Fontana Santos Alves⁴⁰, S. Ghosh⁴⁰, A. Gilbert⁴⁰, R. Granier de Cassagnac⁴⁰, A. Hakimi⁴⁰, B. Harikrishnan⁴⁰, L. Kalipoliti⁴⁰, G. Liu⁴⁰, M. Nguyen⁴⁰, C. Ochando⁴⁰, R. Salerno⁴⁰, J. B. Sauvan⁴⁰, Y. Sirois⁴⁰, L. Urda Gómez⁴⁰, E. Vernazza⁴⁰, A. Zabi⁴⁰, A. Zghiche⁴⁰, J.-L. Agram^{41,s}, J. Andrea⁴¹, D. Apparú⁴¹, D. Bloch⁴¹, J.-M. Brom⁴¹, E. C. Chabert⁴¹, C. Collard⁴¹, S. Falke⁴¹, U. Goerlach⁴¹, R. Haerberle⁴¹, A.-C. Le Bihan⁴¹, M. Meena⁴¹, O. Poncet⁴¹, G. Saha⁴¹, M. A. Sessini⁴¹, P. Van Hove⁴¹, P. Vaucelle⁴¹, A. Di Florio⁴², D. Amram⁴³, S. Beauceron⁴³, B. Blancon⁴³, G. Boudoul⁴³, N. Chanon⁴³, D. Contardo⁴³, P. Depasse⁴³, C. Dozen^{43,t}, H. El Mamouni⁴³, J. Fay⁴³, S. Gascon⁴³, M. Gouzevitch⁴³, C. Greenberg⁴³, G. Grenier⁴³, B. Ille⁴³, E. Jourdhuy⁴³, I. B. Laktineh⁴³, M. Lethuillier⁴³, L. Mirabito⁴³, S. Perries⁴³, A. Purohit⁴³, M. Vander Donckt⁴³, P. Verdier⁴³, J. Xiao⁴³, A. Khvedelidze^{44,n}, I. Lomidze⁴⁴, Z. Tsamalaidze^{44,n}, V. Botta⁴⁵, S. Consuegra Rodríguez⁴⁵, L. Feld⁴⁵, K. Klein⁴⁵, M. Lipinski⁴⁵, D. Meuser⁴⁵, A. Pauls⁴⁵, D. Pérez Adán⁴⁵, N. Röwert⁴⁵, M. Teroerde⁴⁵, S. Diekmann⁴⁶, A. Dodonova⁴⁶, N. Eich⁴⁶, D. Eliseev⁴⁶, F. Engelke⁴⁶, J. Erdmann⁴⁶, M. Erdmann⁴⁶, P. Fackeldey⁴⁶, B. Fischer⁴⁶, T. Hebbeker⁴⁶, K. Hoepfner⁴⁶, F. Ivone⁴⁶, A. Jung⁴⁶, M. y. Lee⁴⁶, F. Mausolf⁴⁶, M. Merschmeyer⁴⁶, A. Meyer⁴⁶, S. Mukherjee⁴⁶, D. Noll⁴⁶, F. Nowotny⁴⁶, A. Pozdnyakov⁴⁶, Y. Rath⁴⁶, W. Redjeb⁴⁶, F. Rehm⁴⁶, H. Reithler⁴⁶, V. Sarkisovi⁴⁶, A. Schmidt⁴⁶, C. Seth⁴⁶, A. Sharma⁴⁶, J. L. Spah⁴⁶, A. Stein⁴⁶, F. Torres Da Silva De Araujo^{46,u}, S. Wiedenbeck⁴⁶, S. Zaleski⁴⁶, C. Dziwok⁴⁷, G. Flügge⁴⁷, T. Kress⁴⁷, A. Nowack⁴⁷, O. Pooth⁴⁷, A. Stahl⁴⁷, T. Ziemons⁴⁷, A. Zotz⁴⁷, H. Aarup Petersen⁴⁸, M. Aldaya Martin⁴⁸, J. Alimena⁴⁸, S. Amoroso⁴⁸, Y. An⁴⁸, J. Bach⁴⁸, S. Baxter⁴⁸

M. Bayatmakou⁴⁸, H. Becerril Gonzalez⁴⁸, O. Behnke⁴⁸, A. Belvedere⁴⁸, F. Blekman^{48,v}, K. Borras^{48,w}, A. Campbell⁴⁸, A. Cardini⁴⁸, C. Cheng⁴⁸, F. Colombina⁴⁸, G. Eckerlin⁴⁸, D. Eckstein⁴⁸, L. I. Estevez Banos⁴⁸, E. Gallo^{48,v}, A. Geiser⁴⁸, V. Guglielmi⁴⁸, M. Guthoff⁴⁸, A. Hinzmann⁴⁸, L. Jeppe⁴⁸, B. Kaech⁴⁸, M. Kasemann⁴⁸, C. Kleinwort⁴⁸, R. Kogler⁴⁸, M. Komm⁴⁸, D. Krücker⁴⁸, W. Lange⁴⁸, D. Leyva Pernia⁴⁸, K. Lipka^{48,x}, W. Lohmann^{48,y}, F. Lorkowski⁴⁸, R. Mankel⁴⁸, I.-A. Melzer-Pellmann⁴⁸, M. Mendizabal Morentin⁴⁸, A. B. Meyer⁴⁸, G. Milella⁴⁸, K. Moral Figueroa⁴⁸, A. Mussgiller⁴⁸, L. P. Nair⁴⁸, J. Niedziela⁴⁸, A. Nürnberg⁴⁸, Y. Otari⁴⁸, J. Park⁴⁸, E. Ranken⁴⁸, A. Raspereza⁴⁸, D. Rastorguev⁴⁸, J. Rübenach⁴⁸, L. Rygaard⁴⁸, A. Saggio⁴⁸, M. Scham^{48,z,w}, S. Schnake^{48,w}, P. Schütze⁴⁸, C. Schwanenberger^{48,v}, D. Selivanova⁴⁸, K. Sharko⁴⁸, M. Shchedrolosiev⁴⁸, D. Stafford⁴⁸, F. Vazzoler⁴⁸, A. Ventura Barroso⁴⁸, R. Walsh⁴⁸, D. Wang⁴⁸, Q. Wang⁴⁸, K. Wichmann⁴⁸, L. Wiens^{48,w}, C. Wissing⁴⁸, Y. Yang⁴⁸, A. Zimmermann Castro Santos⁴⁸, A. Albrecht⁴⁹, S. Albrecht⁴⁹, M. Antonello⁴⁹, S. Bein⁴⁹, S. Bollweg⁴⁹, M. Bonanomi⁴⁹, P. Connor⁴⁹, K. El Morabit⁴⁹, Y. Fischer⁴⁹, E. Garutti⁴⁹, A. Grohsjean⁴⁹, J. Haller⁴⁹, D. Hundhausen⁴⁹, H. R. Jabusch⁴⁹, G. Kasieczka⁴⁹, P. Keicher⁴⁹, R. Klanner⁴⁹, W. Korcaric⁴⁹, T. Kramer⁴⁹, C. c. Kuo⁴⁹, V. Kutzner⁴⁹, F. Labe⁴⁹, J. Lange⁴⁹, A. Lobanov⁴⁹, C. Matthies⁴⁹, L. Moureaux⁴⁹, M. Mrowietz⁴⁹, A. Nigamova⁴⁹, Y. Nissan⁴⁹, A. Paasch⁴⁹, K. J. Pena Rodriguez⁴⁹, T. Quadfasel⁴⁹, B. Raciti⁴⁹, M. Rieger⁴⁹, D. Savoie⁴⁹, J. Schindler⁴⁹, P. Schleper⁴⁹, M. Schröder⁴⁹, J. Schwandt⁴⁹, M. Sommerhalder⁴⁹, H. Stadie⁴⁹, G. Steinbrück⁴⁹, A. Tews⁴⁹, B. Wiederspan⁴⁹, M. Wolf⁴⁹, S. Brommer⁵⁰, E. Butz⁵⁰, T. Chwalek⁵⁰, A. Dierlamm⁵⁰, A. Droll⁵⁰, U. Elicabuk⁵⁰, N. Faltermann⁵⁰, M. Giffels⁵⁰, A. Gottmann⁵⁰, F. Hartmann^{50,aa}, R. Hofsaess⁵⁰, M. Horzela⁵⁰, U. Husemann⁵⁰, J. Kieseler⁵⁰, M. Klute⁵⁰, R. Koppenhöfer⁵⁰, O. Lavoryk⁵⁰, J. M. Lawhorn⁵⁰, M. Link⁵⁰, A. Lintuluoto⁵⁰, S. Maier⁵⁰, S. Mitra⁵⁰, M. Mormile⁵⁰, Th. Müller⁵⁰, M. Neukum⁵⁰, M. Oh⁵⁰, E. Pfeffer⁵⁰, M. Presilla⁵⁰, G. Quast⁵⁰, K. Rabbertz⁵⁰, B. Regnery⁵⁰, N. Shadskiy⁵⁰, I. Shvetsov⁵⁰, H. J. Simonis⁵⁰, L. Sowa⁵⁰, L. Stockmeier⁵⁰, K. Tauqeer⁵⁰, M. Toms⁵⁰, N. Trevisani⁵⁰, R. F. Von Cube⁵⁰, M. Wassmer⁵⁰, S. Wieland⁵⁰, F. Wittig⁵⁰, R. Wolf⁵⁰, X. Zuo⁵⁰, G. Anagnostou⁵¹, G. Daskalakis⁵¹, A. Kyriakis⁵¹, A. Papadopoulos^{51,aa}, A. Stakia⁵¹, P. Kontaxakis⁵², G. Melachroinos⁵², Z. Painesis⁵², I. Papavergou⁵², I. Paraskevas⁵², N. Saoulidou⁵², K. Theofilatos⁵², E. Tziaferi⁵², K. Vellidis⁵², I. Zisopoulos⁵², G. Bakas⁵³, T. Chatzistavrou⁵³, G. Karapostoli⁵³, K. Kousouris⁵³, I. Papakrivopoulos⁵³, E. Siamarkou⁵³, G. Tsiopolitis⁵³, A. Zacharopoulou⁵³, I. Bestintzanos⁵⁴, I. Evangelou⁵⁴, C. Foudas⁵⁴, C. Kamtsikis⁵⁴, P. Katsoulis⁵⁴, P. Kokkas⁵⁴, P. G. Kosmoglou Kioseoglou⁵⁴, N. Manthos⁵⁴, I. Papadopoulos⁵⁴, J. Strologas⁵⁴, C. Hajdu⁵⁵, D. Horvath^{55,bb,cc}, K. Márton⁵⁵, A. J. Rádl^{55,dd}, F. Sikler⁵⁵, V. Veszpremi⁵⁵, M. Csanád⁵⁶, K. Farkas⁵⁶, A. Fehérkúti^{56,ee}, M. M. A. Gadallah^{56,ff}, Á. Kadlecsek⁵⁶, P. Major⁵⁶, G. Pásztor⁵⁶, G. I. Veres⁵⁶, B. Ujvari⁵⁷, G. Zilizi⁵⁷, G. Bencze⁵⁸, S. Czellar⁵⁸, J. Molnar⁵⁸, Z. Szillasi⁵⁸, T. Csorgo^{59,ee}, F. Nemes^{59,ee}, T. Novak⁵⁹, S. Bansal⁶⁰, S. B. Beri⁶⁰, V. Bhatnagar⁶⁰, G. Chaudhary⁶⁰, S. Chauhan⁶⁰, N. Dhingra^{60,gg}, A. Kaur⁶⁰, A. Kaur⁶⁰, H. Kaur⁶⁰, M. Kaur⁶⁰, S. Kumar⁶⁰, T. Sheokand⁶⁰, J. B. Singh⁶⁰, A. Singla⁶⁰, A. Ahmed⁶¹, A. Bhardwaj⁶¹, A. Chhetri⁶¹, B. C. Choudhary⁶¹, A. Kumar⁶¹, A. Kumar⁶¹, M. Naimuddin⁶¹, K. Ranjan⁶¹, M. K. Saini⁶¹, S. Saumya⁶¹, S. Baradia⁶², S. Barman^{62,hh}, S. Bhattacharya⁶², S. Das Gupta⁶², S. Dutta⁶², S. Dutta⁶², S. Sarkar⁶², M. M. Ameen⁶³, P. K. Behera⁶³, S. C. Behera⁶³, S. Chatterjee⁶³, G. Dash⁶³, P. Jana⁶³, P. Kalbhor⁶³, S. Kamble⁶³, J. R. Komaragiri^{63,ii}, D. Kumar^{63,ii}, T. Mishra⁶³, B. Parida^{63,jj}, P. R. Pujahari⁶³, N. R. Saha⁶³, A. Sharma⁶³, A. K. Sikdar⁶³, R. K. Singh⁶³, P. Verma⁶³, S. Verma⁶³, A. Vijay⁶³, S. Dugad⁶⁴, G. B. Mohanty⁶⁴, M. Shelake⁶⁴, P. Suryadevara⁶⁴, A. Bala⁶⁵, S. Banerjee⁶⁵, R. M. Chatterjee⁶⁵, M. Guchait⁶⁵, Sh. Jain⁶⁵, A. Jaiswal⁶⁵, S. Kumar⁶⁵, G. Majumder⁶⁵, K. Mazumdar⁶⁵, S. Parolia⁶⁵, A. Thachayath⁶⁵, S. Bahinipati^{66,kk}, C. Kar⁶⁶, D. Maity^{66,ll}, P. Mal⁶⁶, V. K. Muraleedharan Nair Bindhu^{66,ll}, K. Naskar^{66,ll}, A. Nayak^{66,ll}, S. Nayak⁶⁶, K. Pal⁶⁶, P. Sadangi⁶⁶, S. K. Swain⁶⁶, S. Varghese^{66,ll}, D. Vats^{66,ll}, S. Acharya^{67,mm}, A. Alpana⁶⁷, S. Dube⁶⁷, B. Gomber^{67,mm}, P. Hazarika⁶⁷, B. Kansal⁶⁷, A. Laha⁶⁷, B. Sahu^{67,mm}, S. Sharma⁶⁷, K. Y. Vaish⁶⁷, H. Bakhshiansohi^{68,nn}, A. Jafari^{68,oo}, M. Zeinali^{68,pp}, S. Bashiri⁶⁹, S. Chenarani^{69,qq}, S. M. Etesami⁶⁹, Y. Hosseini⁶⁹, M. Khakzad⁶⁹, E. Khazaie⁶⁹, M. Mohammadi Najafabadi⁶⁹, S. Tizchang^{69,rr}, M. Felcini⁷⁰, M. Grunewald⁷⁰, M. Abbrescia^{71a,71b}, A. Colaleo^{71a,71b}, D. Creanza^{71a,71c}, B. D'Anzi^{71a,71b}, N. De Filippis^{71a,71c}, M. De Palma^{71a,71b}, W. Elmetenawee^{71a,71b,ss}, N. Ferrara^{71a,71b}, L. Fiore^{71a}, G. Iaselli^{71a,71c}, L. Longo^{71a}, M. Louka^{71a,71b}, G. Maggi^{71a,71c}, M. Maggi^{71a}, I. Margjeka^{71a}, V. Mastrapasqua^{71a,71b}, S. My^{71a,71b}, S. Nuzzo^{71a,71b}, A. Pellicchia^{71a,71b}, A. Pompili^{71a,71b}, G. Pugliese^{71a,71c}, R. Radogna^{71a,71b}, D. Ramos^{71a}, A. Ranieri^{71a}

L. Silvestris^{71a} F. M. Simone^{71a,71c} Ü. Sözbilir^{71a} A. Stamerra^{71a,71b} D. Troiano^{71a,71b} R. Venditti^{71a,71b}
P. Verwilligen^{71a} A. Zaza^{71a,71b} G. Abbiendi^{72a} C. Battilana^{72a,72b} D. Bonacorsi^{72a,72b} P. Capiluppi^{72a,72b}
A. Castro^{72a,72b,a} F. R. Cavallo^{72a} M. Cuffiani^{72a,72b} G. M. Dallavalle^{72a} T. Diotallevi^{72a,72b} F. Fabbri^{72a}
A. Fanfani^{72a,72b} D. Fasanella^{72a} P. Giacomelli^{72a} L. Giommi^{72a,72b} C. Grandi^{72a} L. Guiducci^{72a,72b}
S. Lo Meo^{72a,tt} M. Lorusso^{72a,72b} L. Lunerti^{72a} S. Marcellini^{72a} G. Masetti^{72a} F. L. Navarra^{72a,72b}
G. Paggi^{72a,72b} A. Perrotta^{72a} F. Primavera^{72a,72b} A. M. Rossi^{72a,72b} S. Rossi Tisbeni^{72a,72b} T. Rovelli^{72a,72b}
G. P. Siroli^{72a,72b} S. Costa^{73a,73b,uu} A. Di Mattia^{73a} A. Lapertosa^{73a} R. Potenza^{73a,73b} A. Tricomi^{73a,73b,uu}
C. Tuve^{73a,73b} P. Assiouras^{74a} G. Barbagli^{74a} G. Bardelli^{74a,74b} B. Camaiani^{74a,74b} A. Cassese^{74a}
R. Ceccarelli^{74a} V. Ciulli^{74a,74b} C. Civinini^{74a} R. D' Alessandro^{74a,74b} E. Focardi^{74a,74b} T. Kello^{74a}
G. Latino^{74a,74b} P. Lenzi^{74a,74b} M. Lizzo^{74a} M. Meschini^{74a} S. Paoletti^{74a} A. Papanastassiou^{74a,74b}
G. Sguazzoni^{74a} L. Viliani^{74a} L. Benussi⁷⁵ S. Bianco⁷⁵ S. Meola^{75,vv} D. Piccolo⁷⁵ M. Alves Gallo Pereira^{76a}
F. Ferro^{76a} E. Robutti^{76a} S. Tosi^{76a,76b} A. Benaglia^{77a} F. Brivio^{77a} F. Cetorelli^{77a,77b} F. De Guio^{77a,77b}
M. E. Dinardo^{77a,77b} P. Dini^{77a} S. Gennai^{77a} R. Gerosa^{77a,77b} A. Ghezzi^{77a,77b} P. Govoni^{77a,77b} L. Guzzi^{77a}
M. T. Lucchini^{77a,77b} M. Malberti^{77a} S. Malvezzi^{77a} A. Massironi^{77a} D. Menasce^{77a} L. Moroni^{77a}
M. Paganoni^{77a,77b} S. Palluotto^{77a,77b} D. Pedrini^{77a} A. Perego^{77a,77b} B. S. Pinolini^{77a} G. Pizzati^{77a,77b}
S. Ragazzi^{77a,77b} T. Tabarelli de Fatis^{77a,77b} S. Buontempo^{78a} A. Cagnotta^{78a,78b} F. Carnevali^{78a,78b}
N. Cavallo^{78a,78c} F. Fabozzi^{78a,78c} A. O. M. Iorio^{78a,78b} L. Lista^{78a,78b,ww} P. Paolucci^{78a,aa} B. Rossi^{78a}
R. Ardino^{79a} P. Azzi^{79a} N. Bacchetta^{79a,xx} D. Bisello^{79a,79b} P. Bortignon^{79a} G. Bortolato^{79a,79b}
A. Bragagnolo^{79a,79b} A. C. M. Bulla^{79a} R. Carlin^{79a,79b} P. Checchia^{79a} T. Dorigo^{79a,yy} S. Fantinel^{79a}
F. Fanzago^{79a} U. Gasparini^{79a,79b} S. Giorgetti^{79a} E. Lusiani^{79a} M. Margoni^{79a,79b} M. Migliorini^{79a,79b}
J. Pazzini^{79a,79b} P. Ronchese^{79a,79b} R. Rossin^{79a,79b} F. Simonetto^{79a,79b} M. Tosi^{79a,79b} A. Triossi^{79a,79b}
S. Ventura^{79a} M. Zanetti^{79a,79b} P. Zotto^{79a,79b} A. Zucchetta^{79a,79b} G. Zumerle^{79a,79b} A. Braghieri^{80a}
S. Calzaferri^{80a} D. Fiorina^{80a} P. Montagna^{80a,80b} V. Re^{80a} C. Riccardi^{80a,80b} P. Salvini^{80a} I. Vai^{80a,80b}
P. Vitulo^{80a,80b} S. Ajmal^{81a,81b} M. E. Ascioti^{81a,81b} G. M. Bilei^{81a} C. Carrivale^{81a,81b} D. Ciangottini^{81a,81b}
L. Fanò^{81a,81b} M. Magherini^{81a,81b} V. Mariani^{81a,81b} M. Menichelli^{81a} F. Moscatelli^{81a,zz} A. Rossi^{81a,81b}
A. Santocchia^{81a,81b} D. Spiga^{81a} T. Tedeschi^{81a,81b} C. Aimè^{82a} C. A. Alexe^{82a,82c} P. Asenov^{82a,82b}
P. Azzurri^{82a} G. Bagliesi^{82a} R. Bhattacharya^{82a} L. Bianchini^{82a,82b} T. Boccali^{82a} E. Bossini^{82a}
D. Bruschini^{82a,82c} R. Castaldi^{82a} M. A. Ciocci^{82a,82b} M. Cipriani^{82a,82b} V. D' Amante^{82a,82d} R. Dell' Orso^{82a}
S. Donato^{82a} A. Giassi^{82a} F. Ligabue^{82a,82c} A. C. Marini^{82a} D. Matos Figueiredo^{82a} A. Messineo^{82a,82b}
S. Mishra^{82a} M. Musich^{82a,82b} F. Palla^{82a} A. Rizzi^{82a,82b} G. Rolandi^{82a,82c} S. Roy Chowdhury^{82a} T. Sarkar^{82a}
A. Scribano^{82a} P. Spagnolo^{82a} R. Tenchini^{82a} G. Tonelli^{82a,82b} N. Turini^{82a,82d} F. Vaselli^{82a,82c} A. Venturi^{82a}
P. G. Verdini^{82a} C. Baldenegro Barrera^{83a,83b} P. Barria^{83a} C. Basile^{83a,83b} F. Cavallari^{83a}
L. Cunqueiro Mendez^{83a,83b} D. Del Re^{83a,83b} E. Di Marco^{83a,83b} M. Diemoz^{83a} F. Errico^{83a,83b} R. Gargiulo^{83a,83b}
E. Longo^{83a,83b} L. Martikainen^{83a,83b} J. Mijuskovic^{83a,83b} G. Organtini^{83a,83b} F. Pandolfi^{83a} R. Paramatti^{83a,83b}
C. Quaranta^{83a,83b} S. Rahatlou^{83a,83b} C. Rovelli^{83a} F. Santanastasio^{83a,83b} L. Soffi^{83a} V. Vladimirov^{83a,83b}
N. Amapane^{84a,84b} R. Arcidiacono^{84a,84c} S. Argiro^{84a,84b} M. Arneodo^{84a,84c} N. Bartosik^{84a} R. Bellan^{84a,84b}
A. Bellora^{84a,84b} C. Biino^{84a} C. Borca^{84a,84b} N. Cartiglia^{84a} M. Costa^{84a,84b} R. Covarelli^{84a,84b} N. Demaria^{84a}
L. Finco^{84a} M. Grippo^{84a,84b} B. Kiani^{84a,84b} F. Legger^{84a} F. Luongo^{84a,84b} C. Mariotti^{84a} L. Markovic^{84a,84b}
S. Maselli^{84a} A. Mecca^{84a,84b} L. Menzio^{84a,84b} P. Meridiani^{84a} E. Migliore^{84a,84b} M. Monteno^{84a} R. Mulargia^{84a}
M. M. Obertino^{84a,84b} G. Ortona^{84a} L. Pacher^{84a,84b} N. Pastrone^{84a} M. Pelliccioni^{84a} M. Ruspa^{84a,84c}
F. Siviero^{84a,84b} V. Sola^{84a,84b} A. Solano^{84a,84b} A. Staiano^{84a} C. Tarricone^{84a,84b} D. Trocino^{84a}
G. Umoret^{84a,84b} R. White^{84a,84b} J. Babbar^{85a,85b} S. Belforte^{85a} V. Candelise^{85a,85b} M. Casarsa^{85a}
F. Cossutti^{85a} K. De Leo^{85a} G. Della Ricca^{85a,85b} S. Dogra⁸⁶ J. Hong⁸⁶ B. Kim⁸⁶ J. Kim⁸⁶ D. Lee⁸⁶
H. Lee⁸⁶ S. W. Lee⁸⁶ C. S. Moon⁸⁶ Y. D. Oh⁸⁶ M. S. Ryu⁸⁶ S. Sekmen⁸⁶ B. Tae⁸⁶ Y. C. Yang⁸⁶
M. S. Kim⁸⁷ G. Bak⁸⁸ P. Gwak⁸⁸ H. Kim⁸⁸ D. H. Moon⁸⁸ E. Asilar⁸⁹ J. Choi^{89,aaa} D. Kim⁸⁹ T. J. Kim⁸⁹
J. A. Merlin⁸⁹ Y. Ryou⁸⁹ S. Choi⁹⁰ S. Han⁹⁰ B. Hong⁹⁰ K. Lee⁹⁰ K. S. Lee⁹⁰ S. Lee⁹⁰ J. Yoo⁹⁰ J. Goh⁹¹
S. Yang⁹¹ H. S. Kim⁹² Y. Kim⁹² S. Lee⁹² J. Almond⁹³ J. H. Bhyun⁹³ J. Choi⁹³ J. Choi⁹³ W. Jun⁹³ J. Kim⁹³
Y. W. Kim⁹³ S. Ko⁹³ H. Kwon⁹³ H. Lee⁹³ J. Lee⁹³ J. Lee⁹³ B. H. Oh⁹³ S. B. Oh⁹³ H. Seo⁹³ U. K. Yang⁹³
I. Yoon⁹³ W. Jang⁹⁴ D. Y. Kang⁹⁴ Y. Kang⁹⁴ S. Kim⁹⁴ B. Ko⁹⁴ J. S. H. Lee⁹⁴ Y. Lee⁹⁴ I. C. Park⁹⁴ Y. Roh⁹⁴

I. J. Watson⁹⁴, S. Ha⁹⁵, K. Hwang⁹⁵, H. D. Yoo⁹⁵, M. Choi⁹⁶, M. R. Kim⁹⁶, H. Lee⁹⁶, Y. Lee⁹⁶, I. Yu⁹⁶,
 T. Beyrouthy⁹⁷, Y. Gharbia⁹⁷, F. Alazemi⁹⁸, K. Dreimanis⁹⁹, A. Gaile⁹⁹, C. Munoz Diaz⁹⁹, D. Osite⁹⁹,
 G. Pikurs⁹⁹, A. Potrebko⁹⁹, M. Seidel⁹⁹, D. Sidiropoulos Kontos⁹⁹, N. R. Strautnieks¹⁰⁰, M. Ambrozas¹⁰¹,
 A. Juodagalvis¹⁰¹, A. Rinkevicius¹⁰¹, G. Tamulaitis¹⁰¹, I. Yusuff^{102,bbb}, Z. Zolkapli¹⁰², J. F. Benitez¹⁰³,
 A. Castaneda Hernandez¹⁰³, H. A. Encinas Acosta¹⁰³, L. G. Gallegos Marfinez¹⁰³, M. León Coello¹⁰³,
 J. A. Murillo Quijada¹⁰³, A. Sehrawat¹⁰³, L. Valencia Palomo¹⁰³, G. Ayala¹⁰⁴, H. Castilla-Valdez¹⁰⁴,
 H. Crotte Ledesma¹⁰⁴, E. De La Cruz-Burelo¹⁰⁴, I. Heredia-De La Cruz^{104,ccc}, R. Lopez-Fernandez¹⁰⁴,
 J. Mejia Guisao¹⁰⁴, C. A. Mondragon Herrera¹⁰⁴, A. Sánchez Hernández¹⁰⁴, C. Oropeza Barrera¹⁰⁵,
 D. L. Ramirez Guadarrama¹⁰⁵, M. Ramírez García¹⁰⁵, I. Bautista¹⁰⁶, I. Pedraza¹⁰⁶, H. A. Salazar Ibarguen¹⁰⁶,
 C. Uribe Estrada¹⁰⁶, I. Bujanja¹⁰⁷, N. Raicevic¹⁰⁷, P. H. Butler¹⁰⁸, A. Ahmad¹⁰⁹, M. I. Asghar¹⁰⁹, A. Awais¹⁰⁹,
 M. I. M. Awan¹⁰⁹, H. R. Hoorani¹⁰⁹, W. A. Khan¹⁰⁹, V. Avati¹¹⁰, L. Grzanka¹¹⁰, M. Malawski¹¹⁰, H. Bialkowska¹¹¹,
 M. Bluj¹¹¹, M. Górski¹¹¹, M. Kazana¹¹¹, M. Szleper¹¹¹, P. Zalewski¹¹¹, K. Bunkowski¹¹², K. Doroba¹¹²,
 A. Kalinowski¹¹², M. Konecki¹¹², J. Krolikowski¹¹², A. Muhammad¹¹², P. Fokow¹¹³, K. Pozniak¹¹³,
 W. Zablotny¹¹³, M. Araujo¹¹⁴, D. Bastos¹¹⁴, C. Beirão Da Cruz E Silva¹¹⁴, A. Boletti¹¹⁴, M. Bozzo¹¹⁴,
 T. Camporesi¹¹⁴, G. Da Molin¹¹⁴, P. Faccioli¹¹⁴, M. Gallinaro¹¹⁴, J. Hollar¹¹⁴, N. Leonardo¹¹⁴,
 G. B. Marozzo¹¹⁴, A. Petrilli¹¹⁴, M. Pisano¹¹⁴, J. Seixas¹¹⁴, J. Varela¹¹⁴, J. W. Wulff¹¹⁴, P. Adzic¹¹⁵,
 P. Milenovic¹¹⁵, D. Devetak¹¹⁶, M. Dordevic¹¹⁶, J. Milosevic¹¹⁶, L. Nadder¹¹⁶, V. Rekovic¹¹⁶,
 J. Alcaraz Maestre¹¹⁷, Cristina F. Bedoya¹¹⁷, J. A. Brochero Cifuentes¹¹⁷, Oliver M. Carretero¹¹⁷, M. Cepeda¹¹⁷,
 M. Cerrada¹¹⁷, N. Colino¹¹⁷, B. De La Cruz¹¹⁷, A. Delgado Peris¹¹⁷, A. Escalante Del Valle¹¹⁷,
 D. Fernández Del Val¹¹⁷, J. P. Fernández Ramos¹¹⁷, J. Flix¹¹⁷, M. C. Fouz¹¹⁷, O. Gonzalez Lopez¹¹⁷,
 S. Goy Lopez¹¹⁷, J. M. Hernandez¹¹⁷, M. I. Josa¹¹⁷, J. Llorente Merino¹¹⁷, E. Martin Viscasillas¹¹⁷, D. Moran¹¹⁷,
 C. M. Morcillo Perez¹¹⁷, Á. Navarro Tobar¹¹⁷, C. Perez Dengra¹¹⁷, A. Pérez-Calero Yzquierdo¹¹⁷,
 J. Puerta Pelayo¹¹⁷, I. Redondo¹¹⁷, S. Sánchez Navas¹¹⁷, J. Sastre¹¹⁷, J. Vazquez Escobar¹¹⁷, J. F. de Trocóniz¹¹⁸,
 B. Alvarez Gonzalez¹¹⁹, J. Cuevas¹¹⁹, J. Fernandez Menendez¹¹⁹, S. Folgueras¹¹⁹, I. Gonzalez Caballero¹¹⁹,
 P. Leguina¹¹⁹, E. Palencia Cortezon¹¹⁹, J. Prado Pico¹¹⁹, C. Ramón Álvarez¹¹⁹, V. Rodríguez Bouza¹¹⁹,
 A. Soto Rodríguez¹¹⁹, A. Trapote¹¹⁹, C. Vico Villalba¹¹⁹, P. Vischia¹¹⁹, S. Bhowmik¹²⁰, S. Blanco Fernández¹²⁰,
 I. J. Cabrillo¹²⁰, A. Calderon¹²⁰, J. Duarte Campderros¹²⁰, M. Fernandez¹²⁰, G. Gomez¹²⁰, C. Lasasoa García¹²⁰,
 R. Lopez Ruiz¹²⁰, C. Martinez Rivero¹²⁰, P. Martinez Ruiz del Arbol¹²⁰, F. Matorras¹²⁰, P. Matorras Cuevas¹²⁰,
 E. Navarrete Ramos¹²⁰, J. Piedra Gomez¹²⁰, L. Scodellaro¹²⁰, I. Vila¹²⁰, J. M. Vizan Garcia¹²⁰,
 B. Kailasapathy^{121,ddd}, D. D. C. Wickramarathna¹²¹, W. G. D. Dharmaratna^{122,eee}, K. Liyanage¹²², N. Perera¹²²,
 D. Abbaneo¹²³, C. Amendola¹²³, E. Auffray¹²³, G. Auzinger¹²³, J. Baechler¹²³, D. Barney¹²³,
 A. Bermúdez Martínez¹²³, M. Bianco¹²³, A. A. Bin Anuar¹²³, A. Bocci¹²³, L. Borgonovi¹²³, C. Botta¹²³,
 E. Brondolin¹²³, C. Caillol¹²³, G. Cerminara¹²³, N. Chernyavskaya¹²³, D. d'Enterria¹²³, A. Dabrowski¹²³,
 A. David¹²³, A. De Roeck¹²³, M. M. Defranchis¹²³, M. Deile¹²³, M. Dobson¹²³, G. Franzoni¹²³, W. Funk¹²³,
 S. Giani¹²³, D. Gigi¹²³, K. Gill¹²³, F. Glege¹²³, J. Hegeman¹²³, J. K. Heikkilä¹²³, B. Huber¹²³, V. Innocente¹²³,
 T. James¹²³, P. Janot¹²³, O. Kaluzinska¹²³, O. Karacheban^{123,y}, S. Laurila¹²³, P. Lecoq¹²³, E. Leutgeb¹²³,
 C. Lourenço¹²³, L. Malgeri¹²³, M. Mannelli¹²³, M. Matthewman¹²³, A. Mehta¹²³, F. Meijers¹²³, S. Mersi¹²³,
 E. Meschi¹²³, V. Milosevic¹²³, F. Monti¹²³, F. Moortgat¹²³, M. Mulders¹²³, I. Neutelings¹²³, S. Orfanelli¹²³,
 F. Pantaleo¹²³, G. Petrucciani¹²³, A. Pfeiffer¹²³, M. Pierini¹²³, H. Qu¹²³, D. Rabady¹²³, B. Ribeiro Lopes¹²³,
 F. Riti¹²³, M. Rovere¹²³, H. Sakulin¹²³, R. Salvatico¹²³, S. Sanchez Cruz¹²³, S. Scarfi¹²³, C. Schwick¹²³,
 M. Selvaggi¹²³, A. Sharma¹²³, K. Shchelina¹²³, P. Silva¹²³, P. Sphicas^{123,fff}, A. G. Stahl Leitner¹²³, A. Steen¹²³,
 S. Summers¹²³, D. Treille¹²³, P. Tropea¹²³, D. Walter¹²³, J. Wanczyk^{123,ggg}, J. Wang¹²³, K. A. Wozniak^{123,hhh},
 S. Wuchterl¹²³, P. Zehetner¹²³, P. Zejdl¹²³, W. D. Zeuner¹²³, T. Bevilacqua^{124,iii}, L. Caminada^{124,iii},
 A. Ebrahimi¹²⁴, W. Erdmann¹²⁴, R. Horisberger¹²⁴, Q. Ingram¹²⁴, H. C. Kaestli¹²⁴, D. Kotlinski¹²⁴, C. Lange¹²⁴,
 M. Missiroli^{124,iii}, L. Noehte^{124,iii}, T. Rohe¹²⁴, A. Samalan¹²⁴, T. K. Aarrestad¹²⁵, M. Backhaus¹²⁵,
 G. Bonomelli¹²⁵, A. Calandri¹²⁵, C. Cazzaniga¹²⁵, K. Datta¹²⁵, P. De Bryas Dexmiers D'archiac^{125,ggg},
 A. De Cosa¹²⁵, G. Dissertori¹²⁵, M. Dittmar¹²⁵, M. Donegà¹²⁵, F. Eble¹²⁵, M. Galli¹²⁵, K. Gedia¹²⁵,
 F. Glessgen¹²⁵, C. Grab¹²⁵, N. Härringer¹²⁵, T. G. Harte¹²⁵, D. Hits¹²⁵, W. Lustermann¹²⁵, A.-M. Lyon¹²⁵,
 R. A. Manzoni¹²⁵, M. Marchegiani¹²⁵, L. Marchese¹²⁵, C. Martin Perez¹²⁵, A. Mascellani^{125,ggg}

F. Nessi-Tedaldi¹²⁵, F. Pauss¹²⁵, V. Perovic¹²⁵, S. Pigazzini¹²⁵, B. Ristic¹²⁵, R. Seidita¹²⁵, J. Steggemann^{125,ggg},
A. Tarabini¹²⁵, D. Valsecchi¹²⁵, R. Wallny¹²⁵, C. Amsler^{126,jjj}, P. Bärtshi¹²⁶, M. F. Canelli¹²⁶, K. Cormier¹²⁶,
M. Huwiler¹²⁶, W. Jin¹²⁶, A. Jofrehei¹²⁶, B. Kilminster¹²⁶, S. Leontsinis¹²⁶, S. P. Liechti¹²⁶, A. Macchiolo¹²⁶,
P. Meiring¹²⁶, F. Meng¹²⁶, J. Motta¹²⁶, A. Reimers¹²⁶, P. Robmann¹²⁶, M. Senger¹²⁶, E. Shokr¹²⁶, F. Stäger¹²⁶,
R. Tramontano¹²⁶, C. Adloff^{127,kkk}, D. Bhowmik¹²⁷, C. M. Kuo¹²⁷, W. Lin¹²⁷, P. K. Rout¹²⁷, P. C. Tiwari^{127,ii},
L. Ceard¹²⁸, K. F. Chen¹²⁸, Z. g. Chen¹²⁸, A. De Iorio¹²⁸, W.-S. Hou¹²⁸, T. h. Hsu¹²⁸, Y. w. Kao¹²⁸, S. Karmakar¹²⁸,
G. Kole¹²⁸, Y. y. Li¹²⁸, R.-S. Lu¹²⁸, E. Paganis¹²⁸, X. f. Su¹²⁸, J. Thomas-Wilsker¹²⁸, L. s. Tsai¹²⁸, D. Tsiouou¹²⁸,
H. y. Wu¹²⁸, E. Yazgan¹²⁸, C. Asawatangtrakuldee¹²⁹, N. Srimanobhas¹²⁹, V. Wachirapusanand¹²⁹, D. Agyel¹³⁰,
F. Boran¹³⁰, F. Dolek¹³⁰, I. Dumanoglu^{130,lll}, E. Eskut¹³⁰, Y. Guler^{130,mmm}, E. Gurpinar Guler^{130,mmm}, C. Isik¹³⁰,
O. Kara¹³⁰, A. Kayis Topaksu¹³⁰, U. Kiminsu¹³⁰, Y. Komurcu¹³⁰, G. Onengut¹³⁰, K. Ozdemir^{130,nnn}, A. Polatoz¹³⁰,
B. Tali^{130,ooo}, U. G. Tok¹³⁰, S. Turkcapar¹³⁰, E. Uslan¹³⁰, I. S. Zorbakir¹³⁰, G. Sokmen¹³¹, M. Yalvac^{131,ppp},
B. Akgun¹³², I. O. Atakisi¹³², E. Gülmez¹³², M. Kaya^{132,qqq}, O. Kaya^{132,rrr}, S. Tekten^{132,sss}, A. Cakir¹³³,
K. Cankocak^{133,lll,ttt}, G. G. Dincer^{133,lll}, S. Sen^{133,uuu}, O. Aydilek^{134,vvv}, B. Hacisahinoglu¹³⁴, I. Hos^{134,www},
B. Kaynak¹³⁴, S. Ozkorucuklu¹³⁴, O. Potok¹³⁴, H. Sert¹³⁴, C. Simsek¹³⁴, C. Zorbilmez¹³⁴, S. Cerci¹³⁵,
B. Isildak^{135,xxx}, D. Sunar Cerci¹³⁵, T. Yetkin¹³⁵, A. Boyaryntsev¹³⁶, B. Grynyov¹³⁶, L. Levchuk¹³⁷,
D. Anthony¹³⁸, J. J. Brooke¹³⁸, A. Bundock¹³⁸, F. Bury¹³⁸, E. Clement¹³⁸, D. Cussans¹³⁸, H. Flacher¹³⁸,
M. Glowacki¹³⁸, J. Goldstein¹³⁸, H. F. Heath¹³⁸, M.-L. Holmberg¹³⁸, L. Kreczko¹³⁸, S. Paramesvaran¹³⁸,
L. Robertshaw¹³⁸, V. J. Smith¹³⁸, K. Walkingshaw Pass¹³⁸, A. H. Ball¹³⁹, K. W. Bell¹³⁹, A. Belyaev^{139,yyy}, C. Brew¹³⁹,
R. M. Brown¹³⁹, D. J. A. Cockerill¹³⁹, C. Cooke¹³⁹, A. Elliot¹³⁹, K. V. Ellis¹³⁹, K. Harder¹³⁹, S. Harper¹³⁹,
J. Linacre¹³⁹, K. Manolopoulos¹³⁹, D. M. Newbold¹³⁹, E. Olaiya¹³⁹, D. Petyt¹³⁹, T. Reis¹³⁹, A. R. Sahasransu¹³⁹,
G. Salvi¹³⁹, T. Schuh¹³⁹, C. H. Shepherd-Themistocleous¹³⁹, I. R. Tomalin¹³⁹, K. C. Whalen¹³⁹, T. Williams¹³⁹,
I. Andreou¹⁴⁰, R. Bainbridge¹⁴⁰, P. Bloch¹⁴⁰, C. E. Brown¹⁴⁰, O. Buchmuller¹⁴⁰, C. A. Carrillo Montoya¹⁴⁰,
G. S. Chahal^{140,zzz}, D. Colling¹⁴⁰, J. S. Dancu¹⁴⁰, I. Das¹⁴⁰, P. Dauncey¹⁴⁰, G. Davies¹⁴⁰, M. Della Negra¹⁴⁰,
S. Fayer¹⁴⁰, G. Fedi¹⁴⁰, G. Hall¹⁴⁰, A. Howard¹⁴⁰, G. Iles¹⁴⁰, C. R. Knight¹⁴⁰, P. Krueper¹⁴⁰, J. Langford¹⁴⁰,
K. H. Law¹⁴⁰, J. León Holgado¹⁴⁰, L. Lyons¹⁴⁰, A.-M. Magnan¹⁴⁰, B. Maier¹⁴⁰, S. Mallios¹⁴⁰,
M. Mieskolainen¹⁴⁰, J. Nash^{140,aaaa}, M. Pesaresi¹⁴⁰, P. B. Pradeep¹⁴⁰, B. C. Radburn-Smith¹⁴⁰, A. Richards¹⁴⁰,
A. Rose¹⁴⁰, K. Savva¹⁴⁰, C. Seez¹⁴⁰, R. Shukla¹⁴⁰, A. Tapper¹⁴⁰, K. Uchida¹⁴⁰, G. P. Uttley¹⁴⁰, T. Virdee^{140,aa},
M. Vojinovic¹⁴⁰, N. Wardle¹⁴⁰, D. Winterbottom¹⁴⁰, J. E. Cole¹⁴¹, A. Khan¹⁴¹, P. Kyberd¹⁴¹, I. D. Reid¹⁴¹,
S. Abdullin¹⁴², A. Brinkerhoff¹⁴², E. Collins¹⁴², M. R. Darwish¹⁴², J. Dittmann¹⁴², K. Hatakeyama¹⁴²,
J. Hiltbrand¹⁴², B. McMaster¹⁴², J. Samudio¹⁴², S. Sawant¹⁴², C. Sutantawibul¹⁴², J. Wilson¹⁴², R. Bartek¹⁴³,
A. Dominguez¹⁴³, A. E. Simsek¹⁴³, S. S. Yu¹⁴³, B. Bam¹⁴⁴, A. Buchot Perraguin¹⁴⁴, R. Chudasama¹⁴⁴,
S. I. Cooper¹⁴⁴, C. Crovella¹⁴⁴, S. V. Gleyzer¹⁴⁴, E. Pearson¹⁴⁴, C. U. Perez¹⁴⁴, P. Rumerio^{144,bbbb}, E. Usai¹⁴⁴,
R. Yi¹⁴⁴, A. Akpinar¹⁴⁵, C. Cosby¹⁴⁵, G. De Castro¹⁴⁵, Z. Demiragli¹⁴⁵, C. Erice¹⁴⁵, C. Fangmeier¹⁴⁵,
C. Fernandez Madrazo¹⁴⁵, E. Fontanesi¹⁴⁵, D. Gastler¹⁴⁵, F. Golf¹⁴⁵, S. Jeon¹⁴⁵, J. O'cain¹⁴⁵, I. Reed¹⁴⁵,
J. Rohlf¹⁴⁵, K. Salyer¹⁴⁵, D. Sperka¹⁴⁵, D. Spitzbart¹⁴⁵, I. Suarez¹⁴⁵, A. Tsatsos¹⁴⁵, A. G. Zecchinelli¹⁴⁵,
G. Barone¹⁴⁶, G. Benelli¹⁴⁶, D. Cutts¹⁴⁶, L. Gouskos¹⁴⁶, M. Hadley¹⁴⁶, U. Heintz¹⁴⁶, J. M. Hogan^{146,cccc},
T. Kwon¹⁴⁶, G. Landsberg¹⁴⁶, K. T. Lau¹⁴⁶, D. Li¹⁴⁶, J. Luo¹⁴⁶, S. Mondal¹⁴⁶, T. Russell¹⁴⁶, S. Sagir^{146,dddd},
X. Shen¹⁴⁶, F. Simpson¹⁴⁶, M. Stamenkovic¹⁴⁶, N. Venkatasubramanian¹⁴⁶, X. Yan¹⁴⁶, S. Abbott¹⁴⁷, B. Barton¹⁴⁷,
C. Brainerd¹⁴⁷, R. Breedon¹⁴⁷, H. Cai¹⁴⁷, M. Calderon De La Barca Sanchez¹⁴⁷, M. Chertok¹⁴⁷, M. Citron¹⁴⁷,
J. Conway¹⁴⁷, P. T. Cox¹⁴⁷, R. Erbacher¹⁴⁷, F. Jensen¹⁴⁷, O. Kukral¹⁴⁷, G. Mocellin¹⁴⁷, M. Mulhearn¹⁴⁷,
S. Ostrom¹⁴⁷, W. Wei¹⁴⁷, S. Yoo¹⁴⁷, F. Zhang¹⁴⁷, K. Adamidis¹⁴⁸, M. Bachtis¹⁴⁸, D. Campos¹⁴⁸, R. Cousins¹⁴⁸,
A. Datta¹⁴⁸, G. Flores Avila¹⁴⁸, J. Hauser¹⁴⁸, M. Ignatenko¹⁴⁸, M. A. Iqbal¹⁴⁸, T. Lam¹⁴⁸, Y. f. Lo¹⁴⁸,
E. Manca¹⁴⁸, A. Nunez Del Prado¹⁴⁸, D. Saltzberg¹⁴⁸, V. Valuev¹⁴⁸, R. Clare¹⁴⁹, J. W. Gary¹⁴⁹, G. Hanson¹⁴⁹,
A. Aportela¹⁵⁰, A. Arora¹⁵⁰, J. G. Branson¹⁵⁰, S. Cittolin¹⁵⁰, S. Cooperstein¹⁵⁰, D. Diaz¹⁵⁰, J. Duarte¹⁵⁰,
L. Giannini¹⁵⁰, Y. Gu¹⁵⁰, J. Guiang¹⁵⁰, R. Kansal¹⁵⁰, V. Krutelyov¹⁵⁰, R. Lee¹⁵⁰, J. Letts¹⁵⁰,
M. Masciovecchio¹⁵⁰, F. Mokhtar¹⁵⁰, S. Mukherjee¹⁵⁰, M. Pieri¹⁵⁰, M. Quinnan¹⁵⁰, B. V. Sathia Narayanan¹⁵⁰,
V. Sharma¹⁵⁰, M. Tadel¹⁵⁰, E. Vourliotis¹⁵⁰, F. Würthwein¹⁵⁰, Y. Xiang¹⁵⁰, A. Yagil¹⁵⁰, A. Barzdukas¹⁵¹,
L. Brennan¹⁵¹, C. Campagnari¹⁵¹, K. Downham¹⁵¹, C. Grieco¹⁵¹, J. Incandela¹⁵¹, J. Kim¹⁵¹, A. J. Li¹⁵¹,
P. Masterson¹⁵¹, H. Mei¹⁵¹, J. Richman¹⁵¹, S. N. Santpur¹⁵¹, U. Sarica¹⁵¹, R. Schmitz¹⁵¹, F. Setti¹⁵¹

J. Sheplock¹⁵¹, D. Stuart¹⁵¹, T. Á. Vámi¹⁵¹, S. Wang¹⁵¹, D. Zhang¹⁵¹, S. Bhattacharya¹⁵², A. Bornheim¹⁵², O. Cerri¹⁵², A. Latorre¹⁵², J. Mao¹⁵², H. B. Newman¹⁵², G. Reales Gutiérrez¹⁵², M. Spiropulu¹⁵², J. R. Vlimant¹⁵², C. Wang¹⁵², S. Xie¹⁵², R. Y. Zhu¹⁵², J. Alison¹⁵³, S. An¹⁵³, P. Bryant¹⁵³, M. Cremonesi¹⁵³, V. Dutta¹⁵³, T. Ferguson¹⁵³, T. A. Gómez Espinosa¹⁵³, A. Harilal¹⁵³, A. Kallil Tharayil¹⁵³, C. Liu¹⁵³, T. Mudholkar¹⁵³, S. Murthy¹⁵³, P. Palit¹⁵³, K. Park¹⁵³, M. Paulini¹⁵³, A. Roberts¹⁵³, A. Sanchez¹⁵³, W. Terrill¹⁵³, J. P. Cumalat¹⁵⁴, W. T. Ford¹⁵⁴, A. Hart¹⁵⁴, A. Hassani¹⁵⁴, G. Karathanasis¹⁵⁴, N. Manganelli¹⁵⁴, J. Pearkes¹⁵⁴, C. Savard¹⁵⁴, N. Schonbeck¹⁵⁴, K. Stenson¹⁵⁴, K. A. Ulmer¹⁵⁴, S. R. Wagner¹⁵⁴, N. Zipper¹⁵⁴, D. Zuolo¹⁵⁴, J. Alexander¹⁵⁵, S. Bright-Thonney¹⁵⁵, X. Chen¹⁵⁵, D. J. Cranshaw¹⁵⁵, J. Fan¹⁵⁵, X. Fan¹⁵⁵, S. Hogan¹⁵⁵, P. Kotamnives¹⁵⁵, J. Monroy¹⁵⁵, M. Oshiro¹⁵⁵, J. R. Patterson¹⁵⁵, M. Reid¹⁵⁵, A. Ryd¹⁵⁵, J. Thom¹⁵⁵, P. Wittich¹⁵⁵, R. Zou¹⁵⁵, M. Albrow¹⁵⁶, M. Alyari¹⁵⁶, O. Amram¹⁵⁶, G. Apollinari¹⁵⁶, A. Apresyan¹⁵⁶, L. A. T. Bauerdick¹⁵⁶, D. Berry¹⁵⁶, J. Berryhill¹⁵⁶, P. C. Bhat¹⁵⁶, K. Burkett¹⁵⁶, J. N. Butler¹⁵⁶, A. Canepa¹⁵⁶, G. B. Cerati¹⁵⁶, H. W. K. Cheung¹⁵⁶, F. Chlebana¹⁵⁶, G. Cummings¹⁵⁶, J. Dickinson¹⁵⁶, I. Dutta¹⁵⁶, V. D. Elvira¹⁵⁶, Y. Feng¹⁵⁶, J. Freeman¹⁵⁶, A. Gandrakota¹⁵⁶, Z. Gecse¹⁵⁶, L. Gray¹⁵⁶, D. Green¹⁵⁶, A. Grummer¹⁵⁶, S. Grünendahl¹⁵⁶, D. Guerrero¹⁵⁶, O. Gutsche¹⁵⁶, R. M. Harris¹⁵⁶, R. Heller¹⁵⁶, T. C. Herwig¹⁵⁶, J. Hirschauer¹⁵⁶, B. Jayatilaka¹⁵⁶, S. Jindariani¹⁵⁶, M. Johnson¹⁵⁶, U. Joshi¹⁵⁶, T. Klijnsma¹⁵⁶, B. Klima¹⁵⁶, K. H. M. Kwok¹⁵⁶, S. Lammel¹⁵⁶, C. Lee¹⁵⁶, D. Lincoln¹⁵⁶, R. Lipton¹⁵⁶, T. Liu¹⁵⁶, C. Madrid¹⁵⁶, K. Maeshima¹⁵⁶, C. Mantilla¹⁵⁶, D. Mason¹⁵⁶, P. McBride¹⁵⁶, P. Merkel¹⁵⁶, S. Mrenna¹⁵⁶, S. Nahn¹⁵⁶, J. Ngadiuba¹⁵⁶, D. Noonan¹⁵⁶, S. Norberg¹⁵⁶, V. Papadimitriou¹⁵⁶, N. Pastika¹⁵⁶, K. Pedro¹⁵⁶, C. Pena^{156,eeee}, F. Ravera¹⁵⁶, A. Reinsvold Hall^{156,ffff}, L. Ristori¹⁵⁶, M. Safdari¹⁵⁶, E. Sexton-Kennedy¹⁵⁶, N. Smith¹⁵⁶, A. Soha¹⁵⁶, L. Spiegel¹⁵⁶, S. Stoynev¹⁵⁶, J. Strait¹⁵⁶, L. Taylor¹⁵⁶, S. Tkaczyk¹⁵⁶, N. V. Tran¹⁵⁶, L. Uplegger¹⁵⁶, E. W. Vaandering¹⁵⁶, I. Zoi¹⁵⁶, C. Aruta¹⁵⁷, P. Avery¹⁵⁷, D. Bourilkov¹⁵⁷, P. Chang¹⁵⁷, V. Cherepanov¹⁵⁷, R. D. Field¹⁵⁷, C. Huh¹⁵⁷, E. Koenig¹⁵⁷, M. Kolosova¹⁵⁷, J. Konigsberg¹⁵⁷, A. Korytov¹⁵⁷, K. Matchev¹⁵⁷, N. Menendez¹⁵⁷, G. Mitselmakher¹⁵⁷, K. Mohrman¹⁵⁷, A. Muthirakalayil Madhu¹⁵⁷, N. Rawal¹⁵⁷, S. Rosenzweig¹⁵⁷, Y. Takahashi¹⁵⁷, J. Wang¹⁵⁷, T. Adams¹⁵⁸, A. Al Kadhimi¹⁵⁸, A. Askew¹⁵⁸, S. Bower¹⁵⁸, R. Hashmi¹⁵⁸, R. S. Kim¹⁵⁸, S. Kim¹⁵⁸, T. Kolberg¹⁵⁸, G. Martinez¹⁵⁸, H. Prosper¹⁵⁸, P. R. Prova¹⁵⁸, M. Wulansatiti¹⁵⁸, R. Yohay¹⁵⁸, J. Zhang¹⁵⁸, B. Alsufyani¹⁵⁹, M. M. Baarmand¹⁵⁹, S. Butalla¹⁵⁹, S. Das¹⁵⁹, T. Elkafrawy^{159,q}, M. Hohlmann¹⁵⁹, E. Yanes¹⁵⁹, M. R. Adams¹⁶⁰, A. Baty¹⁶⁰, C. Bennett¹⁶⁰, R. Cavanaugh¹⁶⁰, R. Escobar Franco¹⁶⁰, O. Evdokimov¹⁶⁰, C. E. Gerber¹⁶⁰, M. Hawksworth¹⁶⁰, A. Hingrajiya¹⁶⁰, D. J. Hofman¹⁶⁰, J. h. Lee¹⁶⁰, D. S. Lemos¹⁶⁰, A. H. Merrit¹⁶⁰, C. Mills¹⁶⁰, S. Nanda¹⁶⁰, G. Oh¹⁶⁰, B. Ozek¹⁶⁰, D. Pilipovic¹⁶⁰, R. Pradhan¹⁶⁰, E. Prifti¹⁶⁰, T. Roy¹⁶⁰, S. Rudrabhatla¹⁶⁰, N. Singh¹⁶⁰, M. B. Tonjes¹⁶⁰, N. Varelas¹⁶⁰, M. A. Wadud¹⁶⁰, Z. Ye¹⁶⁰, J. Yoo¹⁶⁰, M. Alhousseini¹⁶¹, D. Blend¹⁶¹, K. Dilsiz^{161,gggg}, L. Emediato¹⁶¹, G. Karaman¹⁶¹, O. K. Köseyan¹⁶¹, J.-P. Merlo¹⁶¹, A. Mestvirishvili^{161,hhhh}, O. Neogi¹⁶¹, H. Ogul^{161,iiii}, Y. Onel¹⁶¹, A. Penzo¹⁶¹, C. Snyder¹⁶¹, E. Tiras^{161,jjjj}, B. Blumenfeld¹⁶², L. Corcodilos¹⁶², J. Davis¹⁶², A. V. Gritsan¹⁶², L. Kang¹⁶², S. Kyriacou¹⁶², P. Maksimovic¹⁶², M. Roguljic¹⁶², J. Roskes¹⁶², S. Sekhar¹⁶², M. Swartz¹⁶², A. Abreu¹⁶³, L. F. Alcerro Alcerro¹⁶³, J. Anguiano¹⁶³, S. Arteaga Escatel¹⁶³, P. Baringer¹⁶³, A. Bean¹⁶³, Z. Flowers¹⁶³, D. Grove¹⁶³, J. King¹⁶³, G. Krintiras¹⁶³, M. Lazarovits¹⁶³, C. Le Mahieu¹⁶³, J. Marquez¹⁶³, M. Murray¹⁶³, M. Nickel¹⁶³, M. Pitt¹⁶³, S. Popescu^{163,kkkk}, C. Rogan¹⁶³, C. Royon¹⁶³, S. Sanders¹⁶³, C. Smith¹⁶³, G. Wilson¹⁶³, B. Allmond¹⁶⁴, R. Gujju Gurnadha¹⁶⁴, A. Ivanov¹⁶⁴, K. Kaadze¹⁶⁴, Y. Maravin¹⁶⁴, J. Natoli¹⁶⁴, D. Roy¹⁶⁴, G. Sorrentino¹⁶⁴, A. Baden¹⁶⁵, A. Belloni¹⁶⁵, J. Bistany-riebman¹⁶⁵, Y. M. Chen¹⁶⁵, S. C. Eno¹⁶⁵, N. J. Hadley¹⁶⁵, S. Jabeen¹⁶⁵, R. G. Kellogg¹⁶⁵, T. Koeth¹⁶⁵, B. Kronheim¹⁶⁵, Y. Lai¹⁶⁵, S. Lascio¹⁶⁵, A. C. Mignerey¹⁶⁵, S. Nabili¹⁶⁵, C. Palmer¹⁶⁵, C. Papageorgakis¹⁶⁵, M. M. Paranjpe¹⁶⁵, E. Popova^{165,n}, A. Shevelev¹⁶⁵, L. Wang¹⁶⁵, J. Bendavid¹⁶⁶, I. A. Cali¹⁶⁶, P. c. Chou¹⁶⁶, M. D'Alfonso¹⁶⁶, J. Eysermans¹⁶⁶, C. Freer¹⁶⁶, G. Gomez-Ceballos¹⁶⁶, M. Goncharov¹⁶⁶, G. Grosso¹⁶⁶, P. Harris¹⁶⁶, D. Hoang¹⁶⁶, D. Kovalskiy¹⁶⁶, J. Krupa¹⁶⁶, L. Lavezzo¹⁶⁶, Y.-J. Lee¹⁶⁶, K. Long¹⁶⁶, C. McGinn¹⁶⁶, A. Novak¹⁶⁶, M. I. Park¹⁶⁶, C. Paus¹⁶⁶, C. Reissel¹⁶⁶, C. Roland¹⁶⁶, G. Roland¹⁶⁶, S. Rothman¹⁶⁶, G. S. F. Stephans¹⁶⁶, Z. Wang¹⁶⁶, B. Wyslouch¹⁶⁶, T. J. Yang¹⁶⁶, B. Crossman¹⁶⁷, B. M. Joshi¹⁶⁷, C. Kapsiak¹⁶⁷, M. Krohn¹⁶⁷, D. Mahon¹⁶⁷, J. Mans¹⁶⁷, B. Marzocchi¹⁶⁷, M. Revering¹⁶⁷, R. Rusack¹⁶⁷, R. Saradhy¹⁶⁷, N. Strobbe¹⁶⁷, K. Bloom¹⁶⁸, D. R. Claes¹⁶⁸, G. Haza¹⁶⁸, J. Hossain¹⁶⁸, C. Joo¹⁶⁸, I. Kravchenko¹⁶⁸, J. E. Siado¹⁶⁸, W. Tabb¹⁶⁸, A. Vagnerini¹⁶⁸, A. Wightman¹⁶⁸, F. Yan¹⁶⁸, D. Yu¹⁶⁸, H. Bandyopadhyay¹⁶⁹, L. Hay¹⁶⁹, H. w. Hsia¹⁶⁹

I. Iashvili¹⁶⁹, A. Kalogeropoulos¹⁶⁹, A. Kharchilava¹⁶⁹, M. Morris¹⁶⁹, D. Nguyen¹⁶⁹, S. Rappoccio¹⁶⁹,
 H. Rejeb Sfar¹⁶⁹, A. Williams¹⁶⁹, P. Young¹⁶⁹, G. Alverson¹⁷⁰, E. Barberis¹⁷⁰, J. Bonilla¹⁷⁰, B. Bylsma¹⁷⁰,
 M. Campana¹⁷⁰, J. Dervan¹⁷⁰, Y. Haddad¹⁷⁰, Y. Han¹⁷⁰, I. Israr¹⁷⁰, A. Krishna¹⁷⁰, J. Li¹⁷⁰, M. Lu¹⁷⁰,
 G. Madigan¹⁷⁰, R. Mccarthy¹⁷⁰, D. M. Morse¹⁷⁰, V. Nguyen¹⁷⁰, T. Orimoto¹⁷⁰, A. Parker¹⁷⁰, L. Skinnari¹⁷⁰,
 D. Wood¹⁷⁰, J. Bueghly¹⁷¹, S. Dittmer¹⁷¹, K. A. Hahn¹⁷¹, Y. Liu¹⁷¹, M. Mcginnis¹⁷¹, Y. Miao¹⁷¹, D. G. Monk¹⁷¹,
 M. H. Schmitt¹⁷¹, A. Taliercio¹⁷¹, M. Velasco¹⁷¹, G. Agarwal¹⁷², R. Band¹⁷², R. Bucci¹⁷², S. Castells¹⁷²,
 A. Das¹⁷², R. Goldouzian¹⁷², M. Hildreth¹⁷², K. W. Ho¹⁷², K. Hurtado Anampa¹⁷², T. Ivanov¹⁷², C. Jessop¹⁷²,
 K. Lannon¹⁷², J. Lawrence¹⁷², N. Loukas¹⁷², L. Lutton¹⁷², J. Mariano¹⁷², N. Marinelli¹⁷², I. Mcalister¹⁷²,
 T. McCauley¹⁷², C. Mcgrady¹⁷², C. Moore¹⁷², Y. Musienko^{172,n}, H. Nelson¹⁷², M. Osherson¹⁷², A. Piccinelli¹⁷²,
 R. Ruchti¹⁷², A. Townsend¹⁷², Y. Wan¹⁷², M. Wayne¹⁷², H. Yockey¹⁷², M. Zarucki¹⁷², L. Zygala¹⁷², A. Basnet¹⁷³,
 M. Carrigan¹⁷³, L. S. Durkin¹⁷³, C. Hill¹⁷³, M. Joyce¹⁷³, M. Nunez Ornelas¹⁷³, K. Wei¹⁷³, D. A. Wenzl¹⁷³,
 B. L. Winer¹⁷³, B. R. Yates¹⁷³, H. Bouchamaoui¹⁷⁴, K. Coldham¹⁷⁴, P. Das¹⁷⁴, G. Dezoort¹⁷⁴, P. Elmer¹⁷⁴,
 A. Frankenthal¹⁷⁴, B. Greenberg¹⁷⁴, N. Haubrich¹⁷⁴, K. Kennedy¹⁷⁴, G. Kopp¹⁷⁴, S. Kwan¹⁷⁴, D. Lange¹⁷⁴,
 A. Loeliger¹⁷⁴, D. Marlow¹⁷⁴, I. Ojalvo¹⁷⁴, J. Olsen¹⁷⁴, D. Stickland¹⁷⁴, C. Tully¹⁷⁴, L. H. Vage¹⁷⁴, S. Malik¹⁷⁵,
 R. Sharma¹⁷⁵, A. S. Bakshi¹⁷⁶, S. Chandra¹⁷⁶, R. Chawla¹⁷⁶, A. Gu¹⁷⁶, L. Gutay¹⁷⁶, M. Jones¹⁷⁶, A. W. Jung¹⁷⁶,
 A. M. Koshy¹⁷⁶, M. Liu¹⁷⁶, G. Negro¹⁷⁶, N. Neumeister¹⁷⁶, G. Paspalaki¹⁷⁶, S. Piperov¹⁷⁶, V. Scheurer¹⁷⁶,
 J. F. Schulte¹⁷⁶, M. Stojanovic¹⁷⁶, J. Thieman¹⁷⁶, A. K. Viridi¹⁷⁶, F. Wang¹⁷⁶, A. Wildridge¹⁷⁶, W. Xie¹⁷⁶,
 Y. Yao¹⁷⁶, J. Dolen¹⁷⁷, N. Parashar¹⁷⁷, A. Pathak¹⁷⁷, D. Acosta¹⁷⁸, T. Carnahan¹⁷⁸, K. M. Ecklund¹⁷⁸,
 P. J. Fernández Manteca¹⁷⁸, S. Freed¹⁷⁸, P. Gardner¹⁷⁸, F. J. M. Geurts¹⁷⁸, I. Krommydas¹⁷⁸, W. Li¹⁷⁸, J. Lin¹⁷⁸,
 O. Miguel Colin¹⁷⁸, B. P. Padley¹⁷⁸, R. Redjimi¹⁷⁸, J. Rotter¹⁷⁸, E. Yigitbasi¹⁷⁸, Y. Zhang¹⁷⁸, A. Bodek¹⁷⁹,
 P. de Barbaro¹⁷⁹, R. Demina¹⁷⁹, J. L. Dulemba¹⁷⁹, A. Garcia-Bellido¹⁷⁹, O. Hindrichs¹⁷⁹, A. Khukhunaishvili¹⁷⁹,
 N. Parmar¹⁷⁹, P. Parygin^{179,n}, R. Taus¹⁷⁹, B. Chiarito¹⁸⁰, J. P. Chou¹⁸⁰, S. V. Clark¹⁸⁰, D. Gadkari¹⁸⁰,
 Y. Gershtein¹⁸⁰, E. Halkiadakis¹⁸⁰, M. Heindl¹⁸⁰, C. Houghton¹⁸⁰, D. Jaroslawski¹⁸⁰, S. Konstantinou¹⁸⁰,
 I. Laflotte¹⁸⁰, A. Lath¹⁸⁰, R. Montalvo¹⁸⁰, K. Nash¹⁸⁰, J. Reichert¹⁸⁰, H. Routray¹⁸⁰, P. Saha¹⁸⁰, S. Salur¹⁸⁰,
 S. Schnetzer¹⁸⁰, S. Somalwar¹⁸⁰, R. Stone¹⁸⁰, S. A. Thayil¹⁸⁰, S. Thomas¹⁸⁰, J. Vora¹⁸⁰, H. Wang¹⁸⁰, D. Ally¹⁸¹,
 A. G. Delannoy¹⁸¹, S. Fiorendi¹⁸¹, S. Higginbotham¹⁸¹, T. Holmes¹⁸¹, A. R. Kanuganti¹⁸¹, N. Karunarathna¹⁸¹,
 L. Lee¹⁸¹, E. Nibigira¹⁸¹, S. Spanier¹⁸¹, D. Aebi¹⁸², M. Ahmad¹⁸², T. Akhter¹⁸², K. Androsov^{182,ggg},
 O. Bouhali^{182,llll}, R. Eusebi¹⁸², J. Gilmore¹⁸², T. Huang¹⁸², T. Kamon^{182,mmmm}, H. Kim¹⁸², S. Luo¹⁸²,
 R. Mueller¹⁸², D. Overton¹⁸², D. Rathjens¹⁸², A. Safonov¹⁸², N. Akchurin¹⁸³, J. Damgov¹⁸³, N. Gogate¹⁸³,
 V. Hegde¹⁸³, A. Hussain¹⁸³, Y. Kazhykarim¹⁸³, K. Lamichhane¹⁸³, S. W. Lee¹⁸³, A. Mankel¹⁸³, T. Peltola¹⁸³,
 I. Volobouev¹⁸³, E. Appelt¹⁸⁴, Y. Chen¹⁸⁴, S. Greene¹⁸⁴, A. Gurrola¹⁸⁴, W. Johns¹⁸⁴,
 R. Kunnawalkam Elayavalli¹⁸⁴, A. Melo¹⁸⁴, F. Romeo¹⁸⁴, P. Sheldon¹⁸⁴, S. Tuo¹⁸⁴, J. Velkovska¹⁸⁴,
 J. Viinikainen¹⁸⁴, B. Cardwell¹⁸⁵, H. Chung¹⁸⁵, B. Cox¹⁸⁵, J. Hakala¹⁸⁵, R. Hirosky¹⁸⁵, A. Ledovskoy¹⁸⁵,
 C. Neu¹⁸⁵, S. Bhattacharya¹⁸⁶, P. E. Karchin¹⁸⁶, A. Aravind¹⁸⁷, S. Banerjee¹⁸⁷, K. Black¹⁸⁷, T. Bose¹⁸⁷,
 E. Chavez¹⁸⁷, S. Dasu¹⁸⁷, P. Everaerts¹⁸⁷, C. Galloni¹⁸⁷, H. He¹⁸⁷, M. Herndon¹⁸⁷, A. Herve¹⁸⁷, C. K. Koraka¹⁸⁷,
 A. Lanaro¹⁸⁷, R. Loveless¹⁸⁷, J. Madhusudanan Sreekala¹⁸⁷, A. Mallampalli¹⁸⁷, A. Mohammadi¹⁸⁷, S. Mondal¹⁸⁷,
 G. Parida¹⁸⁷, L. Pétré¹⁸⁷, D. Pinna¹⁸⁷, A. Savin¹⁸⁷, V. Shang¹⁸⁷, V. Sharma¹⁸⁷, W. H. Smith¹⁸⁷, D. Teague¹⁸⁷,
 H. F. Tsoi¹⁸⁷, W. Vetens¹⁸⁷, A. Warden¹⁸⁷, S. Afanasiev¹⁸⁸, V. Alexakhin¹⁸⁸, D. Budkouski¹⁸⁸, I. Golutvin^{188,a},
 I. Gorbunov¹⁸⁸, V. Karjavine¹⁸⁸, V. Korenkov¹⁸⁸, A. Lanev¹⁸⁸, A. Malakhov¹⁸⁸, V. Matveev^{188,n}, V. Palichik¹⁸⁸,
 V. Perelygin¹⁸⁸, M. Savina¹⁸⁸, V. Shalaev¹⁸⁸, S. Shmatov¹⁸⁸, S. Shulha¹⁸⁸, V. Smirnov¹⁸⁸, O. Teryaev¹⁸⁸,
 N. Voytishin¹⁸⁸, B. S. Yuldashev^{188,nnnn}, A. Zarubin¹⁸⁸, I. Zhizhin¹⁸⁸, G. Gavrilo¹⁸⁸, V. Golovtsov¹⁸⁸,
 Y. Ivanov¹⁸⁸, V. Kim^{188,n}, P. Levchenko^{188,oooo}, V. Murzin¹⁸⁸, V. Oreshkin¹⁸⁸, D. Sosnov¹⁸⁸, V. Sulimov¹⁸⁸,
 L. Uvarov¹⁸⁸, A. Vorobyev^{188,a}, Yu. Andreev¹⁸⁸, A. Dermenev¹⁸⁸, S. Gninenko¹⁸⁸, N. Golubev¹⁸⁸,
 A. Karneyeu¹⁸⁸, D. Kirpichnikov¹⁸⁸, M. Kirsanov¹⁸⁸, N. Krasnikov¹⁸⁸, I. Tlisova¹⁸⁸, A. Toropin¹⁸⁸,
 T. Aushev¹⁸⁸, K. Ivanov¹⁸⁸, V. Gavrilo¹⁸⁸, N. Lychkovskaya¹⁸⁸, A. Nikitenko^{188,pppp,qqqq}, V. Popov¹⁸⁸,
 A. Zhokin¹⁸⁸, R. Chistov^{188,n}, M. Danilov^{188,n}, S. Polikarpov^{188,n}, V. Andreev¹⁸⁸, M. Azarkin¹⁸⁸,
 M. Kirakosyan¹⁸⁸, A. Terkulov¹⁸⁸, E. Boos¹⁸⁸, V. Bunichev¹⁸⁸, M. Dubinin^{188,eeee}, L. Dudko¹⁸⁸, A. Ershov¹⁸⁸,
 A. Gribushin¹⁸⁸, V. Klyukhin¹⁸⁸, O. Kodolova^{188,qqqq}, S. Obraztsov¹⁸⁸, S. Petrushanko¹⁸⁸, V. Savrin¹⁸⁸,
 A. Snigirev¹⁸⁸, V. Blinov^{188,n}, T. Dimova^{188,n}, A. Kozyrev^{188,n}, O. Radchenko^{188,n}, Y. Skovpen^{188,n}

V. Kachanov¹⁸⁸, D. Konstantinov¹⁸⁸, S. Slabospitskii¹⁸⁸, A. Uzunian¹⁸⁸, A. Babaev¹⁸⁸,
V. Borshch¹⁸⁸ and D. Druzhkin¹⁸⁸

(CMS Collaboration)

- ¹*Yerevan Physics Institute, Yerevan, Armenia*
²*Institut für Hochenergiephysik, Vienna, Austria*
³*Universiteit Antwerpen, Antwerpen, Belgium*
⁴*Vrije Universiteit Brussel, Brussel, Belgium*
⁵*Université Libre de Bruxelles, Bruxelles, Belgium*
⁶*Ghent University, Ghent, Belgium*
⁷*Université Catholique de Louvain, Louvain-la-Neuve, Belgium*
⁸*Centro Brasileiro de Pesquisas Físicas, Rio de Janeiro, Brazil*
⁹*Universidade do Estado do Rio de Janeiro, Rio de Janeiro, Brazil*
¹⁰*Universidade Estadual Paulista, Universidade Federal do ABC, São Paulo, Brazil*
¹¹*Institute for Nuclear Research and Nuclear Energy, Bulgarian Academy of Sciences, Sofia, Bulgaria*
¹²*University of Sofia, Sofia, Bulgaria*
¹³*Instituto De Alta Investigación, Universidad de Tarapacá, Casilla 7 D, Arica, Chile*
¹⁴*Beihang University, Beijing, China*
¹⁵*Department of Physics, Tsinghua University, Beijing, China*
¹⁶*Institute of High Energy Physics, Beijing, China*
¹⁷*State Key Laboratory of Nuclear Physics and Technology, Peking University, Beijing, China*
¹⁸*Guangdong Provincial Key Laboratory of Nuclear Science and Guangdong-Hong Kong Joint Laboratory of Quantum Matter, South China Normal University, Guangzhou, China*
¹⁹*Sun Yat-Sen University, Guangzhou, China*
²⁰*University of Science and Technology of China, Hefei, China*
²¹*Nanjing Normal University, Nanjing, China*
²²*Institute of Modern Physics and Key Laboratory of Nuclear Physics and Ion-beam Application (MOE) - Fudan University, Shanghai, China*
²³*Zhejiang University, Hangzhou, Zhejiang, China*
²⁴*Universidad de Los Andes, Bogota, Colombia*
²⁵*Universidad de Antioquia, Medellín, Colombia*
²⁶*University of Split, Faculty of Electrical Engineering, Mechanical Engineering and Naval Architecture, Split, Croatia*
²⁷*University of Split, Faculty of Science, Split, Croatia*
²⁸*Institute Rudjer Boskovic, Zagreb, Croatia*
²⁹*University of Cyprus, Nicosia, Cyprus*
³⁰*Charles University, Prague, Czech Republic*
³¹*Escuela Politecnica Nacional, Quito, Ecuador*
³²*Universidad San Francisco de Quito, Quito, Ecuador*
³³*Academy of Scientific Research and Technology of the Arab Republic of Egypt, Egyptian Network of High Energy Physics, Cairo, Egypt*
³⁴*Center for High Energy Physics (CHEP-FU), Fayoum University, El-Fayoum, Egypt*
³⁵*National Institute of Chemical Physics and Biophysics, Tallinn, Estonia*
³⁶*Department of Physics, University of Helsinki, Helsinki, Finland*
³⁷*Helsinki Institute of Physics, Helsinki, Finland*
³⁸*Lappeenranta-Lahti University of Technology, Lappeenranta, Finland*
³⁹*IRFU, CEA, Université Paris-Saclay, Gif-sur-Yvette, France*
⁴⁰*Laboratoire Leprince-Ringuet, CNRS/IN2P3, Ecole Polytechnique, Institut Polytechnique de Paris, Palaiseau, France*
⁴¹*Université de Strasbourg, CNRS, IPHC UMR 7178, Strasbourg, France*
⁴²*Centre de Calcul de l'Institut National de Physique Nucleaire et de Physique des Particules, CNRS/IN2P3, Villeurbanne, France*
⁴³*Institut de Physique des 2 Infinis de Lyon (IP2I), Villeurbanne, France*
⁴⁴*Georgian Technical University, Tbilisi, Georgia*
⁴⁵*RWTH Aachen University, I. Physikalisches Institut, Aachen, Germany*
⁴⁶*RWTH Aachen University, III. Physikalisches Institut A, Aachen, Germany*
⁴⁷*RWTH Aachen University, III. Physikalisches Institut B, Aachen, Germany*
⁴⁸*Deutsches Elektronen-Synchrotron, Hamburg, Germany*
⁴⁹*University of Hamburg, Hamburg, Germany*
⁵⁰*Karlsruher Institut fuer Technologie, Karlsruhe, Germany*

- ⁵¹*Institute of Nuclear and Particle Physics (INPP), NCSR Demokritos, Aghia Paraskevi, Greece*
- ⁵²*National and Kapodistrian University of Athens, Athens, Greece*
- ⁵³*National Technical University of Athens, Athens, Greece*
- ⁵⁴*University of Ioánnina, Ioánnina, Greece*
- ⁵⁵*HUN-REN Wigner Research Centre for Physics, Budapest, Hungary*
- ⁵⁶*MTA-ELTE Lendület CMS Particle and Nuclear Physics Group, Eötvös Loránd University, Budapest, Hungary*
- ⁵⁷*Faculty of Informatics, University of Debrecen, Debrecen, Hungary*
- ⁵⁸*HUN-REN ATOMKI - Institute of Nuclear Research, Debrecen, Hungary*
- ⁵⁹*Karoly Robert Campus, MATE Institute of Technology, Gyongyos, Hungary*
- ⁶⁰*Panjab University, Chandigarh, India*
- ⁶¹*University of Delhi, Delhi, India*
- ⁶²*Saha Institute of Nuclear Physics, HBNI, Kolkata, India*
- ⁶³*Indian Institute of Technology Madras, Madras, India*
- ⁶⁴*Tata Institute of Fundamental Research-A, Mumbai, India*
- ⁶⁵*Tata Institute of Fundamental Research-B, Mumbai, India*
- ⁶⁶*National Institute of Science Education and Research, An OCC of Homi Bhabha National Institute, Bhubaneswar, Odisha, India*
- ⁶⁷*Indian Institute of Science Education and Research (IISER), Pune, India*
- ⁶⁸*Isfahan University of Technology, Isfahan, Iran*
- ⁶⁹*Institute for Research in Fundamental Sciences (IPM), Tehran, Iran*
- ⁷⁰*University College Dublin, Dublin, Ireland*
- ^{71a}*INFN Sezione di Bari, Bari, Italy*
- ^{71b}*Università di Bari, Bari, Italy*
- ^{71c}*Politecnico di Bari, Bari, Italy*
- ^{72a}*INFN Sezione di Bologna, Bologna, Italy*
- ^{72b}*Università di Bologna, Bologna, Italy*
- ^{73a}*INFN Sezione di Catania, Catania, Italy*
- ^{73b}*Università di Catania, Catania, Italy*
- ^{74a}*INFN Sezione di Firenze, Firenze, Italy*
- ^{74b}*Università di Firenze, Firenze, Italy*
- ⁷⁵*INFN Laboratori Nazionali di Frascati, Frascati, Italy*
- ^{76a}*INFN Sezione di Genova, Genova, Italy*
- ^{76b}*Università di Genova, Genova, Italy*
- ^{77a}*INFN Sezione di Milano-Bicocca, Milano, Italy*
- ^{77b}*Università di Milano-Bicocca, Milano, Italy*
- ^{78a}*INFN Sezione di Napoli, Napoli, Italy*
- ^{78b}*Università di Napoli 'Federico II', Napoli, Italy*
- ^{78c}*Università della Basilicata, Potenza, Italy*
- ^{78d}*Scuola Superiore Meridionale (SSM), Napoli, Italy*
- ^{79a}*INFN Sezione di Padova, Padova, Italy*
- ^{79b}*Università di Padova, Padova, Italy*
- ^{79c}*Università di Trento, Trento, Italy*
- ^{80a}*INFN Sezione di Pavia, Pavia, Italy*
- ^{80b}*Università di Pavia, Pavia, Italy*
- ^{81a}*INFN Sezione di Perugia, Perugia, Italy*
- ^{81b}*Università di Perugia, Perugia, Italy*
- ^{82a}*INFN Sezione di Pisa, Pisa, Italy*
- ^{82b}*Università di Pisa, Pisa, Italy*
- ^{82c}*Scuola Normale Superiore di Pisa, Pisa, Italy*
- ^{82d}*Università di Siena, Siena, Italy*
- ^{83a}*INFN Sezione di Roma, Roma, Italy*
- ^{83b}*Sapienza Università di Roma, Roma, Italy*
- ^{84a}*INFN Sezione di Torino, Torino, Italy*
- ^{84b}*Università di Torino, Torino, Italy*
- ^{84c}*Università del Piemonte Orientale, Novara, Italy*
- ^{85a}*INFN Sezione di Trieste, Trieste, Italy*
- ^{85b}*Università di Trieste, Trieste, Italy*
- ⁸⁶*Kyungpook National University, Daegu, Korea*
- ⁸⁷*Department of Mathematics and Physics - GWNU, Gangneung, Korea*
- ⁸⁸*Chonnam National University, Institute for Universe and Elementary Particles, Kwangju, Korea*
- ⁸⁹*Hanyang University, Seoul, Korea*

- ⁹⁰*Korea University, Seoul, Korea*
- ⁹¹*Kyung Hee University, Department of Physics, Seoul, Korea*
- ⁹²*Sejong University, Seoul, Korea*
- ⁹³*Seoul National University, Seoul, Korea*
- ⁹⁴*University of Seoul, Seoul, Korea*
- ⁹⁵*Yonsei University, Department of Physics, Seoul, Korea*
- ⁹⁶*Sungkyunkwan University, Suwon, Korea*
- ⁹⁷*College of Engineering and Technology, American University of the Middle East (AUM), Dasman, Kuwait*
- ⁹⁸*Kuwait University - College of Science - Department of Physics, Safat, Kuwait*
- ⁹⁹*Riga Technical University, Riga, Latvia*
- ¹⁰⁰*University of Latvia (LU), Riga, Latvia*
- ¹⁰¹*Vilnius University, Vilnius, Lithuania*
- ¹⁰²*National Centre for Particle Physics, Universiti Malaya, Kuala Lumpur, Malaysia*
- ¹⁰³*Universidad de Sonora (UNISON), Hermosillo, Mexico*
- ¹⁰⁴*Centro de Investigacion y de Estudios Avanzados del IPN, Mexico City, Mexico*
- ¹⁰⁵*Universidad Iberoamericana, Mexico City, Mexico*
- ¹⁰⁶*Benemerita Universidad Autonoma de Puebla, Puebla, Mexico*
- ¹⁰⁷*University of Montenegro, Podgorica, Montenegro*
- ¹⁰⁸*University of Canterbury, Christchurch, New Zealand*
- ¹⁰⁹*National Centre for Physics, Quaid-I-Azam University, Islamabad, Pakistan*
- ¹¹⁰*AGH University of Krakow, Krakow, Poland*
- ¹¹¹*National Centre for Nuclear Research, Swierk, Poland*
- ¹¹²*Institute of Experimental Physics, Faculty of Physics, University of Warsaw, Warsaw, Poland*
- ¹¹³*Warsaw University of Technology, Warsaw, Poland*
- ¹¹⁴*Laboratório de Instrumentação e Física Experimental de Partículas, Lisboa, Portugal*
- ¹¹⁵*Faculty of Physics, University of Belgrade, Belgrade, Serbia*
- ¹¹⁶*VINCA Institute of Nuclear Sciences, University of Belgrade, Belgrade, Serbia*
- ¹¹⁷*Centro de Investigaciones Energéticas Medioambientales y Tecnológicas (CIEMAT), Madrid, Spain*
- ¹¹⁸*Universidad Autónoma de Madrid, Madrid, Spain*
- ¹¹⁹*Universidad de Oviedo, Instituto Universitario de Ciencias y Tecnologías Espaciales de Asturias (ICTEA), Oviedo, Spain*
- ¹²⁰*Instituto de Física de Cantabria (IFCA), CSIC-Universidad de Cantabria, Santander, Spain*
- ¹²¹*University of Colombo, Colombo, Sri Lanka*
- ¹²²*University of Ruhuna, Department of Physics, Matara, Sri Lanka*
- ¹²³*CERN, European Organization for Nuclear Research, Geneva, Switzerland*
- ¹²⁴*PSI Center for Neutron and Muon Sciences, Villigen, Switzerland*
- ¹²⁵*ETH Zurich - Institute for Particle Physics and Astrophysics (IPA), Zurich, Switzerland*
- ¹²⁶*Universität Zürich, Zurich, Switzerland*
- ¹²⁷*National Central University, Chung-Li, Taiwan*
- ¹²⁸*National Taiwan University (NTU), Taipei, Taiwan*
- ¹²⁹*High Energy Physics Research Unit, Department of Physics, Faculty of Science, Chulalongkorn University, Bangkok, Thailand*
- ¹³⁰*Çukurova University, Physics Department, Science and Art Faculty, Adana, Turkey*
- ¹³¹*Middle East Technical University, Physics Department, Ankara, Turkey*
- ¹³²*Bogazici University, Istanbul, Turkey*
- ¹³³*Istanbul Technical University, Istanbul, Turkey*
- ¹³⁴*Istanbul University, Istanbul, Turkey*
- ¹³⁵*Yildiz Technical University, Istanbul, Turkey*
- ¹³⁶*Institute for Scintillation Materials of National Academy of Science of Ukraine, Kharkiv, Ukraine*
- ¹³⁷*National Science Centre, Kharkiv Institute of Physics and Technology, Kharkiv, Ukraine*
- ¹³⁸*University of Bristol, Bristol, United Kingdom*
- ¹³⁹*Rutherford Appleton Laboratory, Didcot, United Kingdom*
- ¹⁴⁰*Imperial College, London, United Kingdom*
- ¹⁴¹*Brunel University, Uxbridge, United Kingdom*
- ¹⁴²*Baylor University, Waco, Texas, USA*
- ¹⁴³*Catholic University of America, Washington, DC, USA*
- ¹⁴⁴*The University of Alabama, Tuscaloosa, Alabama, USA*
- ¹⁴⁵*Boston University, Boston, Massachusetts, USA*
- ¹⁴⁶*Brown University, Providence, Rhode Island, USA*
- ¹⁴⁷*University of California, Davis, Davis, California, USA*
- ¹⁴⁸*University of California, Los Angeles, California, USA*
- ¹⁴⁹*University of California, Riverside, Riverside, California, USA*

- ¹⁵⁰*University of California, San Diego, La Jolla, California, USA*
¹⁵¹*University of California, Santa Barbara - Department of Physics, Santa Barbara, California, USA*
¹⁵²*California Institute of Technology, Pasadena, California, USA*
¹⁵³*Carnegie Mellon University, Pittsburgh, Pennsylvania, USA*
¹⁵⁴*University of Colorado Boulder, Boulder, Colorado, USA*
¹⁵⁵*Cornell University, Ithaca, New York, USA*
¹⁵⁶*Fermi National Accelerator Laboratory, Batavia, Illinois, USA*
¹⁵⁷*University of Florida, Gainesville, Florida, USA*
¹⁵⁸*Florida State University, Tallahassee, Florida, USA*
¹⁵⁹*Florida Institute of Technology, Melbourne, Florida, USA*
¹⁶⁰*University of Illinois Chicago, Chicago, Illinois, USA*
¹⁶¹*The University of Iowa, Iowa City, Iowa, USA*
¹⁶²*Johns Hopkins University, Baltimore, Maryland, USA*
¹⁶³*The University of Kansas, Lawrence, Kansas, USA*
¹⁶⁴*Kansas State University, Manhattan, Kansas, USA*
¹⁶⁵*University of Maryland, College Park, Maryland, USA*
¹⁶⁶*Massachusetts Institute of Technology, Cambridge, Massachusetts, USA*
¹⁶⁷*University of Minnesota, Minneapolis, Minnesota, USA*
¹⁶⁸*University of Nebraska-Lincoln, Lincoln, Nebraska, USA*
¹⁶⁹*State University of New York at Buffalo, Buffalo, New York, USA*
¹⁷⁰*Northeastern University, Boston, Massachusetts, USA*
¹⁷¹*Northwestern University, Evanston, Illinois, USA*
¹⁷²*University of Notre Dame, Notre Dame, Indiana, USA*
¹⁷³*The Ohio State University, Columbus, Ohio, USA*
¹⁷⁴*Princeton University, Princeton, New Jersey, USA*
¹⁷⁵*University of Puerto Rico, Mayaguez, Puerto Rico, USA*
¹⁷⁶*Purdue University, West Lafayette, Indiana, USA*
¹⁷⁷*Purdue University Northwest, Hammond, Indiana, USA*
¹⁷⁸*Rice University, Houston, Texas, USA*
¹⁷⁹*University of Rochester, Rochester, New York, USA*
¹⁸⁰*Rutgers, The State University of New Jersey, Piscataway, New Jersey, USA*
¹⁸¹*University of Tennessee, Knoxville, Tennessee, USA*
¹⁸²*Texas A&M University, College Station, Texas, USA*
¹⁸³*Texas Tech University, Lubbock, Texas, USA*
¹⁸⁴*Vanderbilt University, Nashville, Tennessee, USA*
¹⁸⁵*University of Virginia, Charlottesville, Virginia, USA*
¹⁸⁶*Wayne State University, Detroit, Michigan, USA*
¹⁸⁷*University of Wisconsin - Madison, Madison, Wisconsin, USA*
¹⁸⁸*An institute or international laboratory covered by a cooperation agreement with CERN*

^aDeceased.

^bAlso at Yerevan State University, Yerevan, Armenia.

^cAlso at TU Wien, Vienna, Austria.

^dAlso at Ghent University, Ghent, Belgium.

^eAlso at Universidade do Estado do Rio de Janeiro, Rio de Janeiro, Brazil.

^fAlso at Universidade Estadual de Campinas, Campinas, Brazil.

^gAlso at Federal University of Rio Grande do Sul, Porto Alegre, Brazil.

^hAlso at University of Chinese Academy of Sciences, Beijing, China.

ⁱAlso at China Center of Advanced Science and Technology, Beijing, China.

^jAlso at China Spallation Neutron Source, Guangdong, China.

^kAlso at Henan Normal University, Xinxiang, China.

^lAlso at University of Shanghai for Science and Technology, Shanghai, China.

^mAlso at The University of Iowa, Iowa City, Iowa, USA.

ⁿAlso at another institute or international laboratory covered by a cooperation agreement with CERN.

^oAlso at Zewail City of Science and Technology, Zewail, Egypt.

^pAlso at British University in Egypt, Cairo, Egypt.

^qAlso at Ain Shams University, Cairo, Egypt.

^rAlso at Purdue University, West Lafayette, Indiana, USA.

^sAlso at Université de Haute Alsace, Mulhouse, France.

^tAlso at Istinye University, Istanbul, Turkey.

- ^u Also at The University of the State of Amazonas, Manaus, Brazil.
- ^v Also at University of Hamburg, Hamburg, Germany.
- ^w Also at RWTH Aachen University, III. Physikalisches Institut A, Aachen, Germany.
- ^x Also at Bergische University Wuppertal (BUW), Wuppertal, Germany.
- ^y Also at Brandenburg University of Technology, Cottbus, Germany.
- ^z Also at Forschungszentrum Jülich, Juelich, Germany.
- ^{aa} Also at CERN, European Organization for Nuclear Research, Geneva, Switzerland.
- ^{bb} Also at HUN-REN ATOMKI—Institute of Nuclear Research, Debrecen, Hungary.
- ^{cc} Also at Universitatea Babeş-Bolyai—Facultatea de Fizica, Cluj-Napoca, Romania.
- ^{dd} Also at MTA-ELTE Lendület CMS Particle and Nuclear Physics Group, Eötvös Loránd University, Budapest, Hungary.
- ^{ee} Also at HUN-REN Wigner Research Centre for Physics, Budapest, Hungary.
- ^{ff} Also at Physics Department, Faculty of Science, Assiut University, Assiut, Egypt.
- ^{gg} Also at Punjab Agricultural University, Ludhiana, India.
- ^{hh} Also at University of Visva-Bharati, Santiniketan, India.
- ⁱⁱ Also at Indian Institute of Science (IISc), Bangalore, India.
- ^{jj} Also at Amity University Uttar Pradesh, Noida, India.
- ^{kk} Also at IIT Bhubaneswar, Bhubaneswar, India.
- ^{ll} Also at Institute of Physics, Bhubaneswar, India.
- ^{mm} Also at University of Hyderabad, Hyderabad, India.
- ⁿⁿ Also at Deutsches Elektronen-Synchrotron, Hamburg, Germany.
- ^{oo} Also at Isfahan University of Technology, Isfahan, Iran.
- ^{pp} Also at Sharif University of Technology, Tehran, Iran.
- ^{qq} Also at Department of Physics, University of Science and Technology of Mazandaran, Behshahr, Iran.
- ^{rr} Also at Department of Physics, Faculty of Science, Arak University, ARAK, Iran.
- ^{ss} Also at Helwan University, Cairo, Egypt.
- ^{tt} Also at Italian National Agency for New Technologies, Energy and Sustainable Economic Development, Bologna, Italy.
- ^{uu} Also at Centro Siciliano di Fisica Nucleare e di Struttura Della Materia, Catania, Italy.
- ^{vv} Also at Università degli Studi Guglielmo Marconi, Roma, Italy.
- ^{ww} Also at Scuola Superiore Meridionale, Università di Napoli “Federico II,” Napoli, Italy.
- ^{xx} Also at Fermi National Accelerator Laboratory, Batavia, Illinois, USA.
- ^{yy} Also at Lulea University of Technology, Lulea, Sweden.
- ^{zz} Also at Consiglio Nazionale delle Ricerche—Istituto Officina dei Materiali, Perugia, Italy.
- ^{aaa} Also at Institut de Physique des 2 Infinis de Lyon (IP2I), Villeurbanne, France.
- ^{bbb} Also at Department of Applied Physics, Faculty of Science and Technology, Universiti Kebangsaan Malaysia, Bangi, Malaysia.
- ^{ccc} Also at Consejo Nacional de Ciencia y Tecnología, Mexico City, Mexico.
- ^{ddd} Also at Trincomalee Campus, Eastern University, Sri Lanka, Nilaveli, Sri Lanka.
- ^{eee} Also at Saegis Campus, Nugegoda, Sri Lanka.
- ^{fff} Also at National and Kapodistrian University of Athens, Athens, Greece.
- ^{ggg} Also at Ecole Polytechnique Fédérale Lausanne, Lausanne, Switzerland.
- ^{hhh} Also at University of Vienna, Vienna, Austria.
- ⁱⁱⁱ Also at Universität Zürich, Zurich, Switzerland.
- ^{jjj} Also at Stefan Meyer Institute for Subatomic Physics, Vienna, Austria.
- ^{kkk} Also at Laboratoire d’Annecy-le-Vieux de Physique des Particules, IN2P3-CNRS, Annecy-le-Vieux, France.
- ^{lll} Also at Near East University, Research Center of Experimental Health Science, Mersin, Turkey.
- ^{mmm} Also at Konya Technical University, Konya, Turkey.
- ⁿⁿⁿ Also at Izmir Bakircay University, Izmir, Turkey.
- ^{ooo} Also at Adiyaman University, Adiyaman, Turkey.
- ^{ppp} Also at Bozok Universitetesi Rektörlüğü, Yozgat, Turkey.
- ^{qqq} Also at Marmara University, Istanbul, Turkey.
- ^{rrr} Also at Milli Savunma University, Istanbul, Turkey.
- ^{sss} Also at Kafkas University, Kars, Turkey.
- ^{ttt} Also at Istanbul Okan University, Istanbul, Turkey.
- ^{uuu} Also at Hacettepe University, Ankara, Turkey.
- ^{vvv} Also at Erzincan Binali Yildirim University, Erzincan, Turkey.
- ^{www} Also at Istanbul University—Cerrahpasa, Faculty of Engineering, Istanbul, Turkey.
- ^{xxx} Also at Yildiz Technical University, Istanbul, Turkey.
- ^{yyy} Also at School of Physics and Astronomy, University of Southampton, Southampton, United Kingdom.
- ^{zzz} Also at IPPP Durham University, Durham, United Kingdom.
- ^{aaa} Also at Monash University, Faculty of Science, Clayton, Australia.
- ^{bbb} Also at Università di Torino, Torino, Italy.

- cccc Also at Bethel University, St. Paul, Minnesota, USA.
- dddd Also at Karamanoğlu Mehmetbey University, Karaman, Turkey.
- eeee Also at California Institute of Technology, Pasadena, California, USA.
- ffff Also at United States Naval Academy, Annapolis, Maryland, USA.
- gggg Also at Bingol University, Bingol, Turkey.
- hhhh Also at Georgian Technical University, Tbilisi, Georgia.
- iiii Also at Sinop University, Sinop, Turkey.
- jjjj Also at Erciyes University, Kayseri, Turkey.
- kkkk Also at Horia Hulubei National Institute of Physics and Nuclear Engineering (IFIN-HH), Bucharest, Romania.
- llll Also at Texas A&M University at Qatar, Doha, Qatar.
- mmmm Also at Kyungpook National University, Daegu, Korea.
- nnnn Also at Institute of Nuclear Physics of the Uzbekistan Academy of Sciences, Tashkent, Uzbekistan.
- oooo Also at Northeastern University, Boston, Massachusetts, USA.
- pppp Also at Imperial College, London, United Kingdom.
- qqqq Also at Yerevan Physics Institute, Yerevan, Armenia.